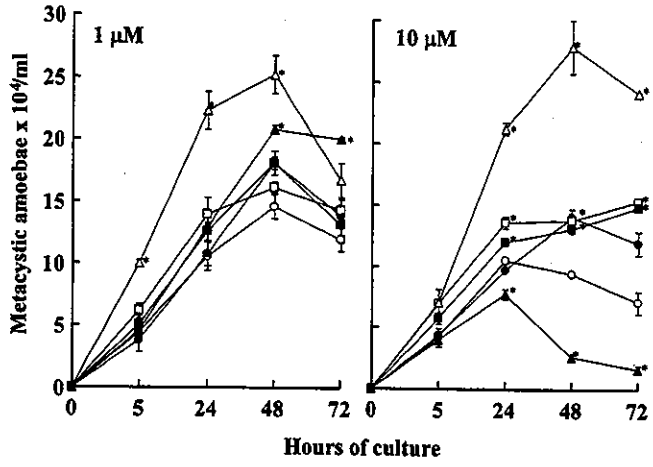

Fig. 3 Effect of cytochalasins on the excystation of *E. invadens*. Cysts were transferred to a growth medium without (*open circles*) and with 1 μM or 10 μM cytochalasin A (*filled circles*), cytochalasin B (*open squares*), dihydrocytochalasin B (*filled squares*), cytochalasin D (*open triangles*) and cytochalasin E (*filled triangles*). The means ± SE of metacystic amoebae for duplicate cultures are plotted (each *asterisk* indicates $P < 0.05$)

Cytochalasin D at 10 μM also markedly increased the number of amoebae from 24 to 72 h compared to the controls, whereas cytochalasins A, B and dihydrocytochalasin B at 10 μM slightly increased the number of amoebae. In contrast, cytochalasin E at 10 μM significantly reduced the number of amoebae from 24 to 72 h compared to the controls.

Discussion

The results indicate that there is a difference in the effect of cytochalasins on the growth and differentiation of *E. invadens*. Only the effect of cytochalasin D on these processes has previously been demonstrated (Makioka et al. 2000, 2001). Since all cytochalasins are cell permeable and there is no report showing any difference in cell permeability among them for a variety of cultured cell types, it is inconceivable that this difference is due to a difference in their permeability. As for the inhibitory effect of cytochalasins on mammalian actin polymerization, which is the primary action common to all cytochalasins, the rate of polymerization of G-actin can be measured by viscometry. The relative inhibitory potency was reported as: cytochalasin D > cytochalasin E = cytochalasin B > dihydrocytochalasin B (Brenner and Korn 1980; Flanagan and Lin 1980). In addition, unlike cytochalasins A and B, cytochalasin D does not inhibit glucose transport, so cytochalasin D has been most widely used to evaluate the function of the actin cytoskeleton. The inhibitory effect of cytochalasin D on growth was very similar to that of our previous study (Makioka et al. 2000), and the results also indicate that cytochalasins B, E, and dihydrocytochalasin B have similar inhibitory effects on growth. In contrast, cytochalasin A had no effect on growth at concentrations of up to 10 μM. Since cytochalasin A is an oxidized form of cytochalasin B (Fig. 4), it is clear that the loss of the inhibitory effect of cytochalasin A is attributable to the oxidized form of oxygen group.

The inhibitory effect of cytochalasin D on encystation is also consistent with our previous results (Makioka et al. 2000). It is clear that cytochalasin D most potently inhibits encystation because, unlike this cytochalasin, other cytochalasins had no inhibitory effect at 1 μM. The results indicate that cytochalasin A, even at 10 μM, had no inhibitory effect on encystation. The reason for this is again attributable to the slight difference in structure between cytochalasins A and B. Since the

Fig. 4 Structural features of cytochalasin A, cytochalasin B, dihydrocytochalasin B, cytochalasin D and cytochalasin E

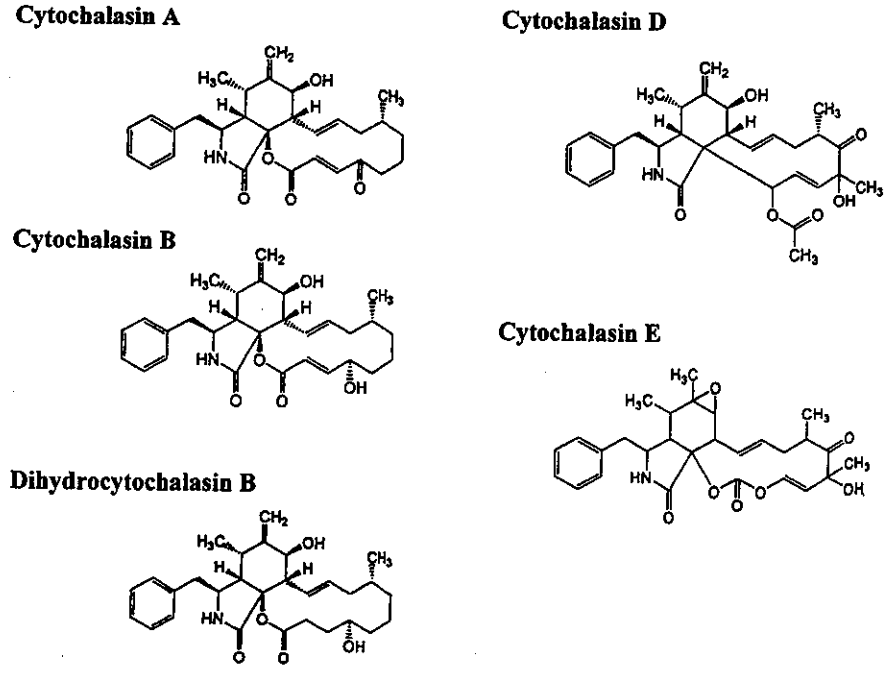

inhibitory effect of dihydrocytochalasin B on encystation was much weaker than that of cytochalasin B, it is conceivable that the absence of a single double bond in dihydrocytochalasin B (Fig. 4) is related to its reduced potency. In this regard, it has been reported that the inhibitory effect of cytochalasin B on sugar transport is lost in dihydrocytochalasin B (Lin et al. 1978).

The results indicate that only cytochalasin D markedly enhances excystation. This suggests that the chemical structure specific for cytochalasin D is related to this effect. Since the central perisohydroindole core rings are common to cytochalasins B and D, a difference in the composition of the attached macrocyclic rings would produce a different effect between the two cytochalasins. The results also show that cytochalasin E, unlike other cytochalasins, has an inhibitory effect on excystation and metacystic development. Since cytochalasin E differs from other cytochalasins by the presence of an epoxide in the central perisohydroindole core ring (Fig. 4), it is conceivable that the epoxide is related to the inhibitory effect of cytochalasin E.

In summary, this study indicates that there are differences in the effect of cytochalasins depending on their chemical structure, which could serve as a useful molecular tool in understanding the structure-activity relationship on the growth and differentiation of *Entamoeba*.

Acknowledgements We thank Dr. N. Watanabe for valuable discussion, Dr. L.S. Diamond for supplying the *Entamoeba invadens* and T. Okita for technical assistance. This work was supported by a Grant-in-Aid for Scientific Research from the Ministry of Education, Culture, Sports and Technology of Japan, and by a Health Science Research Grant for Research on Emerging and Re-emerging Infectious Diseases from the Ministry of Health, Labor and Welfare of Japan.

References

Brenner SL, Korn ED (1980) The effects of cytochalasins on actin polymerization and actin ATPase provide insights into the mechanism of polymerization. J Biol Chem 255:841–844

Bubb MR, Senderowicz AMJ, Sausville EA, Duncan KL, Korn ED (1994) Jasplakinolide, a cytotoxic natural product, induces actin polymerization and competitively inhibits the binding of phalloidin. J Biol Chem 269:14869–14871

Cleveland LR, Sanders EP (1930) Encystation, multiple fission without encystment, excystation, metacystic development, and variation in a pure line and nine strains of *Entamoeba histolytica*. Arch Protistenkd 70:223–266

Diamond LS, Harlow DR, Cunnick CC (1978) A new medium for the axenic cultivation of *Entamoeba histolytica* and other *Entamoeba*. Trans R Soc Trop Med Hyg 72:431–432

Dobell C (1928) Researches on the intestinal protozoa of monkeys and man. Parasitology 20:357–412

Flanagan MD, Lin S (1980) Cytochalasins block actin filament elongation by binding to high affinity sites associated with F-actin. J Biol Chem 255:835–838

Garcia-Zapien A, Hernandez-Gutierrez R, Mora-Galindo J (1995) Simultaneous growth and mass encystations of *Entamoeba invadens* under axenic conditions. Arch Med Res 26:257–262

Geiman QM, Ratcliffe HL (1936) Morphology and life-cycle of an amoeba producing amoebiasis in reptiles. Parasitology 28:208–230

Lin S, Spudich JA (1974) Biochemical studies on the mode of action cytochalasin B. J Biol Chem 249:5778–5783

Lin S, Lin DC, Flanagan MD (1978) Specificity of the effects of cytochalasin B on transport and motile processes. Proc Natl Acad Sci USA 75:329–333

López-Romero E, Villagómez-Castro JC (1993) Encystation in *Entamoeba invadens*. Parasitol Today 9:225–227

Makioka A, Kumagai M, Ohtomo H, Kobayashi S, Takeuchi T (2000) Effect of cytochalasin D on the growth, encystation, and multinucleation of *Entamoeba invadens*. Parasitol Res 86:599–602

Makioka A, Kumagai M, Ohtomo H, Kobayashi S, Takeuchi T (2001) *Entamoeba invadens:* enhancement of excystation and metacystic development by cytochalasin D. Exp Parasitol 98:145–151

Manavanthu EK, Thomas D, Des S (1980) Selectivity of cytochalasin A as a respiratory inhibitor. FEMS Microbiol Lett 7:199–202

McConnachie EW (1955) Studies on *Entamoeba invadens* Rodhain, 1934, in vitro, and its relationship to some other species of *Entamoeba*. Parasitology 45:452–481

Rengpien S, Bailey GB (1975) Differentiation of *Entamoeba*: a new medium and optimal conditions for axenic encystation of *E. invadens*. J Parasitol 61:24–30

Sanchez L, Enea V, Eichinger D (1994) Identification of a developmentally regulated transcript expressed during encystation of *Entamoeba invadens*. Mol Biochem Parasitol 67:125–135

Spector I, Shochet NR, Kashman Y, Groweiss A (1983) Latrunculins: novel marine toxins that disrupt microfilament organization in cultured cells. Science 219:493–495

Parasitol Res (2004) 93: 72–78
DOI 10.1007/s00436-004-1094-8

ORIGINAL PAPER

Laetitia Plaisance · Salah Bouamer · Serge Morand

Description and redescription of *Haliotrema* species (Monogenoidea: Poloyonchoinea: Dactylogyridae) parasitizing butterfly fishes (Teleostei: Chaetodontidae) in the Indo-West Pacific Ocean

Received: 9 February 2004 / Accepted: 11 February 2004 / Published online: 21 April 2004

Abstract *Haliotrema* species are described and/or reported from the gills of butterfly fishes (Chaetodontidae) from coral reefs of the Indo-West Pacific islands: Moorea (French Polynesia), Palau (Micronesia), Wallis (Wallis and Futuna), New Caledonia, Lizard Island and Heron Island (Great Barrier Reef, Australia). *Haliotrema angelopterum* sp. nov., a new species of Monogenoidea parasite from seven species of *Chaetodon* Linnaeus, 1758 (Chaetodontidae), is described. A new redescription and statute are given for *Haliotrema aurigae* (Yamaguti, 1968) comb. nov., a parasite from ten species of *Chaetodon* and one species of *Heniochus* Cuvier, 1816 (Chaetodontidae). New records of *Haliotrema scyphovagina* Yamaguti, 1968 are reported from two localities and from several host species belonging to the genera *Chaetodon* and *Forcipiger* Jordan and McGregor, 1898 (Chaetodontidae).

Introduction

The genus *Haliotrema* (Dactylogyridae, Ancyrocephalinae) was erected by Johnston and Tiegs (1922) for the species *Haliotrema australe* Johnston and Tiegs, 1922, a parasite of the marine black-spotted goat fish, *Upeneus signatus* (Günther, 1867) (Mullidae) (= *Pseudupeneus signatus* Günther, 1867) from Australia. However, Yamaguti (1963), after examining the type species of the genus together with several other species of *Haliotrema*, found many differences relative to the original description and so redescribed the type. Leaning on this new description, Young (1968) made the only major revision of the genus *Haliotrema* with the description of ten new species and an emendation of the diagnosis of the genus.

Since then, *Haliotrema* has become a much expanded taxonomic group which now includes more than 100 species which exhibit very different morphologies and parasitize a large number of hosts with a wide ranging ecology and morphology. This genus is found on teleost fishes from 33 families and belonging to six orders distributed throughout warm seas.

The Monogenoidea parasitizing butterfly fishes (Chaetodontidae) have recently been studied (Plaisance and Kritsky 2004). This study focuses on species belonging to the genera *Euryhaliotrematoides* Plaisance and Kritsky and *Aliatrema* Plaisance and Kritsky.

In the present study, we revise the species of the genus *Haliotrema* parasitizing the Chaetodontidae. We describe *Haliotrema angelopterum* sp. nov., *Pseudohaliotrematoides aurigae* Yamaguti, 1968 is transferred to the genus *Haliotrema*, and new records of *H. scyphovagina* Yamaguti, 1968 from the Indo-West Pacific Ocean are given.

Materials and methods

Thirteen species of butterfly fishes (*Chaetodon auriga* Forsskål, 1775, *C. citrinellus* Cuvier, 1831, *C. ephippium* Cuvier, 1831, *C. kleinii* Bloch, 1790, *C. lunula* (Lacepède, 1802), *C. ornatissimus* Cuvier, 1831, *C. lunulatus* Quoy and Gaimard, 1825, *C. reticulatus* Cuvier, 1831, *C. trifascialis* Quoy and Gaimard, 1825, *C. ulietensis* Cuvier, 1831, *C. vagabundus* Linnaeus, 1758, *Forcipiger flavissimus* Jordan and McGregor, 1898 and *Heniochus chrysostomus* Cuvier, 1831) were collected from six localities in the Indo-West Pacific Ocean (Table 1). The names of the hosts follow those provided in FishBase (Froese and Pauly 2003). Gill baskets were removed from each fish at the site of collection. The gills were placed in hot (60°C) 4% formalin to relax and fix the parasites.

L. Plaisance (✉)
UMR 5555 CNRS-UP, Parasitologie Fonctionelle et Evolutive,
CBTEM, Université, 52 Av. Paul Alduy,
66860 Perpignan, Cedex, France
E-mail: plaisanc@univ-perp.fr
Fax: +33-4-68662281

S. Bouamer · S. Morand
Centre de Biologie et de Gestion des Populations,
Campus International de Baillarguet, CS 30016,
34988 Montferrier-sur-Lez, Cedex, France

Available online at www.sciencedirect.com
SCIENCE DIRECT®
Experimental Parasitology 109 (2005) 27–32
Experimental Parasitology
www.elsevier.com/locate/yexpr

Entamoeba invadens: cysteine protease inhibitors block excystation and metacystic development

Asao Makioka[a,*], Masahiro Kumagai[a], Seiki Kobayashi[b], Tsutomu Takeuchi[b]

[a] *Department of Tropical Medicine, Jikei University School of Medicine, 3-25-8 Nishi-shinbashi, Minato-ku, Tokyo 105-8461, Japan*
[b] *Department of Tropical Medicine and Parasitology, Keio University School of Medicine, 35 Shinanomachi, Shinjuku-ku, Tokyo 160-8582, Japan*

Received 2 June 2004; received in revised form 22 October 2004; accepted 25 October 2004
Available online 9 December 2004

Abstract

We examined the effects of six cysteine protease inhibitors on the excystation and metacystic development of *Entamoeba invadens*. Excystation, which was assessed by counting the number of metacystic amoebae after the induction of excystation, was inhibited by the cysteine protease inhibitors Z-Phe-Ala-DMK and E-64d in a concentration-dependent manner during incubation compared to the controls. Neither inhibitor had a significant effect on cyst viability; thus, their inhibitory effects were not due to the toxic effect on cysts. Metacystic development, when determined by the number of nuclei in amoeba, was also inhibited by these protease inhibitors, because the percentage of 4-nucleate amoebae was higher than in the controls on Day 3 of incubation. Although other cysteine protease inhibitors, Z-Phe-Phe-DMK, E-64, ALLM, and cathepsin inhibitor III, had a weak or little effect on the excystation, they inhibited cysteine protease activity in the lysates of *E. invadens* cysts. Broad bands with gelatinase activity of metacystic amoebae, as well as cysts and trophozoites, were detected in the gelatin substrate gel electrophores and were inhibited by Z-Phe-Ala-DMK. There was a difference in the protease composition between cysts and trophozoites, and the protease composition of metacystic amoebae changed from cyst-type to trophozoite-type during development. These results strongly suggest that cysteine proteases contribute to the excystation and metacystic development of *E. invadens*, which leads to successful infection.

Index Descriptors and Abbreviations: Entamoeba invadens; Protozoa; Cysteine protease; Excystation; Metacystic development; DMSO, dimethyl sulfoxide; DTT, dithiothreitol; SDS–PAGE, sodium dodecyl sulfate–polyacrylamide gel electrophoresis

1. Introduction

Cysteine proteases are not only important virulence factors, but also play a role in the growth and differentiation in many protozoan parasites (McKerrow, 1989; Rosenthal, 1999; Sajid and McKerrow, 2002). This is also true of *Entamoeba histolytica*, because there is accumulating evidence for the potential role of cysteine proteases in the pathogenesis of invasive amebiasis as well as in the growth of the parasites (reviewed by Que and Reed, 2000). In *Entamoeba invadens*, which has been used as a model of encystation and excystation of *E. histolytica*, specific cysteine protease inhibitors significantly reduced the efficiency of encystation, although the effect of inhibition was secondary through decreased trophozoite multiplication (Sharma et al., 1996). However, no studies on the role of cysteine proteases in the excystation and metacystic development of *Entamoeba* have so far been reported.

Excystation and metacystic development are necessary for *Entamoeba* infection, and their processes have been described for *E. histolytica* (Cleveland and Sanders, 1930; Dobell, 1928). Since *E. histolytica* does not encyst

* Corresponding author. Fax: +3 3431 4459.
E-mail address: makioka@jikei.ac.jp (A. Makioka).

0014-4894/$ - see front matter © 2004 Elsevier Inc. All rights reserved.
doi:10.1016/j.exppara.2004.10.003

efficiently in axenic culture, *E. invadens*, a reptilian parasite, has been commonly accepted as a model for the study of encystation and excystation (Eichinger, 1997; López-Romero and Villagómez-Castro, 1993). Excystation is the process through which the whole organism escapes from the cyst through a minute perforation in the cyst wall. Metacystic development is the process in which a hatched metacystic amoeba with four nuclei divides to produce eight amoebulae, which grow to become trophozoites (Cleveland and Sanders, 1930; Dobell, 1928; Geiman and Ratcliffe, 1936). The transfer of *E. invadens* cysts in an encystation medium to a growth medium induces in vitro excystation (Garcia-Zapien et al., 1995; Makioka et al., 2002; McConnachie, 1955; Rengpien and Bailey, 1975). In this study, we examined the effect of cysteine protease inhibitors on the excystation and metacystic development of *E. invadens*. Here, we report that cysteine proteases contribute to these processes of *E. invadens*.

2. Materials and methods

Trophozoites of the IP-1 strain of *E. invadens* were cultured in an axenic growth medium, BI-S-33 (Diamond et al., 1978), at 26 °C. To obtain cysts, trophozoites (5×10^5 cells/ml) were transferred to an encystation medium called 47% LG (LG is BI without glucose; Sanchez et al., 1994). After three days of incubation, the percentage of encystation reached 80% on average. The cells were harvested and treated with 0.05% sarkosyl (Sigma Chemical, St. Louis, MO) to destroy the trophozoites (Sanchez et al., 1994). The remaining cysts were washed with phosphate-buffered saline, counted, and then suspended in a growth medium. The viability of the cysts was determined by trypan blue dye exclusion, and the number of nuclei per cyst was determined after staining with modified Kohn's stain (Kumagai et al., 2001). Cyst preparation included 30% dead or denatured cysts and 70% viable cysts, where 4-nucleate cysts are 30% and 1- to 3-nucleate cysts are 70%. For the experiments on the excystation and metacystic development of *E. invadens*, duplicate cultures of 5×10^5 cysts/ml were incubated with inhibitors for three days. Metacystic amoebae were counted in a hemocytometer on Days 1 and 3, and their viability was determined by trypan blue dye exclusion. Viable metacystic amoebae and cysts were clearly distinguished as light yellow and light blue in color, respectively. The former was also identified by positive motility. The cysteine protease inhibitors used in this study, purchased from Calbiochem (San Diego, CA), are listed in Table 1. These inhibitors were previously used in cultures of human fibroblasts infected with *Toxoplasma gondii* to examine their effect on the intracellular development of parasites (Shaw et al., 2002). All of the inhibitors were dissolved in dimethyl sulfoxide (DMSO).

Table 1
Cysteine protease inhibitors used in the present study

Inhibitor	Specificity
Cysteine protease inhibitors	
Z-Phe-Ala-DMK	Cysteine proteases
Z-Phe-Phe-DMK	Cysteine proteases
E-64	Cysteine proteases
E-64d	Cysteine proteases
Calpain inhibitor 2 (ALLM)	Ca^{2+}-dependent cysteine proteases
Cathepsin (cysteine) protease inhibitor	
Cathepsin inhibitor III	Cathepsin proteases

Abbreviations: Z-Phe-Ala-DMK, Z-Phe-Ala-diazomethylketone; Z-Phe-Phe-DMK, Z-Phe-Phe-diazomethylketone; E-64d, (2S, 3S)-*trans*-epoxysuccinyl-L-leucylamido-3-methylbutane ethylester; E-64, *N*-[*N*-(L-3*trans*-carboxirane-2-carbonyl)-L-leucyl]-agmatine; calpain inhibitor 2, *N*-acetyl-leu-leu-methioninal (ALLM); and cathepsin inhibitor III, Z-Phe-Gly-NHO-Bz-*p*OMe.

The control cultures received the same volume of DMSO.

Metacystic development was determined by the number of nuclei per amoeba. The cells were harvested on Days 1 and 3 in cultures with or without inhibitors and stained with modified Kohn's stain. The number of nuclei per amoeba was determined by the double-counting of least 100 amoebae.

For the assay of cysteine protease activity, cysts (2×10^7/ml) were harvested, washed, and subjected to three freeze–thaw cycles in a phosphate-buffered saline. After centrifugation, the supernatants were obtained as lysates. Protease activity was quantified by the cleavage of synthetic peptide substrate Z-Arg-Arg-AMC (benzyl-oxycarbonyl-arginine-arginine-4-amino-7-methyl-coumarin; Sigma) as previously described (Keene et al., 1986), and recorded as the initial velocity of the cleavage of the fluorescent 4-amino-7-methylcoumarin group/5 µl lysate. The lysates were preincubated for 15 min at room temperature with 10 and 50 µM each of the cysteine protease inhibitors as described above.

Protease gel activity was assessed by gelatin substrate gel electrophoresis as previously described (Keene et al., 1986). The cysts and trophozoites were solubilized using a Laemmli sample buffer (Laemmli, 1970) without a reducing agent, and the supernatants after centrifugation were used. To obtain metacystic amoebae with 4-nuclei and 1-nucleus separately, the cysts were transferred to the growth medium with or without 10 µg/ml aphidicolin (Sigma). The cultures with aphidicolin on Day 1 contained a higher percentage of 4-nucleate amoebae, while the cultures without the drug on Day 3 included that of 1-nucleate amoebae (Makioka et al., 2003). Metacystic amoebae in both cultures were lysed by treatment with a small volume of 0.05% sarkosyl, which had no effect on the cysts. The supernatants after centrifugation were then treated with the Laemmli sample buffer. In certain experiments, trophozoites were treated similarly as for metacystic amoebae. SDS–PAGE was conducted in non-

reducing conditions on 10% gels that had been copolymerized with 0.1% gelatin: equivalent to 5×10^4 loaded per lane. After electrophoresis, the gels was washed for 1 h in 2.5% Triton X-100 to remove SDS, rinsed twice in distilled water, and incubated in 100 mM Tris–HCl (pH 7.4) buffer containing 5 mM EDTA and 2 mM DTT with or without 1 mM Z-Phe-Ala-DMK for 12–18 h at 37 °C. After staining with Coomassie blue and several cycles of destaining, the gelatinase activity was detected as clear bands on the Coomassie blue-stained background of the control gels. All of the experiments of this study were performed at least three times and similar results were obtained. Therefore, the data presented in the results are representative.

3. Results

The effect of cysteine protease inhibitors on the number of metacystic amoebae of *E. invadens* after the transfer of cysts to a growth medium is shown in Fig. 1. Among the inhibitors tested, two cysteine protease inhibitors, Z-Phe-Ala-DMK and E-64d, were effective. For this reason, only the results of these inhibitors are shown. The number of metacystic amoebae in cultures with 10 μM Z-Phe-Ala-DMK during incubation was comparable to the controls, whereas it significantly decreased in cultures with 50 and 100 μM Z-Phe-Ala-DMK compared to the controls. Similarly, metacystic amoebae decreased in number during incubation in cultures with more than 50 μM E-64d. The effects of cysteine protease inhibitors on cyst viability are shown in Fig. 2. The number of viable cysts in the control cultures

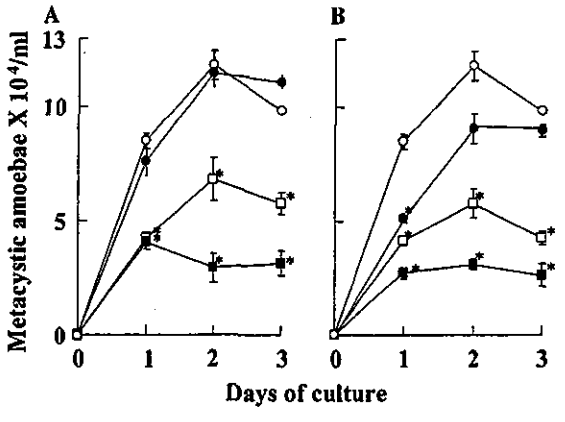

Fig. 1. Effect of cysteine protease inhibitors on the number of metacystic amoebae of *Entamoeba invadens*. Cysts were transferred to a growth medium containing various concentrations of cysteine protease inhibitors Z-Phe-Ala-DMK (A) and E-64d (B). The mean numbers ± SE of metacystic amoebae for the duplicate cultures are plotted (each asterisk indicates $P < 0.05$). Concentrations of 0, 10, 50, and 100 μM are indicated by the white circles, black circles, white squares, and black squares, respectively.

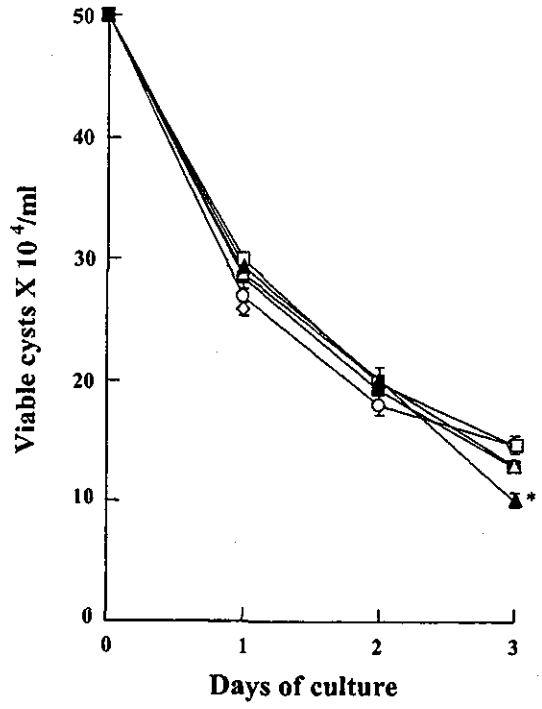

Fig. 2. Effect of cysteine protease inhibitors on the cyst viability of *E. invadens* in the growth medium. The experimental conditions were the same as those for Fig. 1. The mean numbers ± SE of viable cysts for the duplicate cultures are plotted (each asterisk indicates $P < 0.05$). Control (white circles), 50 μM Z-Phe-Ala-DMK (white squares), 100 μM Z-Phe-Ala-DMK (black squares), 50 μM E-64d (white triangles), and 100 μM E-64d (black triangles).

decreased during incubation. It is considered that most immature cysts contained in culture degenerate or die during incubation. The number of viable cysts in cultures containing 50 and 100 μM Z-Phe-Ala-DMK or E-64d during incubation was comparable to or greater than that of the controls, except for 100 μM E-64d on Day 3.

The effects of cysteine protease inhibitors on metacystic development were examined by counting the number of nuclei per cell. As shown in Fig. 3, 9% of the metacystic amoebae were 4-nucleate on Day 1 of incubation in the control cultures, whereas 29 and 34% of the amoebae were in cultures with 100 μM each of Z-Phe-Ala-DMK and E-64d, respectively. The percentage of 4-nucleate amoebae in the control cultures then decreased to 3% on Day 3, following the increased percentages of 1- to 3-nucleate amoebae. In contrast, the percentage of 4-nucleate amoebae in cultures with Z-Phe-Ala-DMK and E-64d was still 19 and 27% on Day 3, respectively, suggesting the inhibition of metacystic development due to these inhibitors.

Since there was a difference in the inhibitory effect on excystation among the cysteine protease inhibitors used, we examined the effects of these inhibitors on cysteine protease activity in cyst lysates. As shown in Fig. 4,

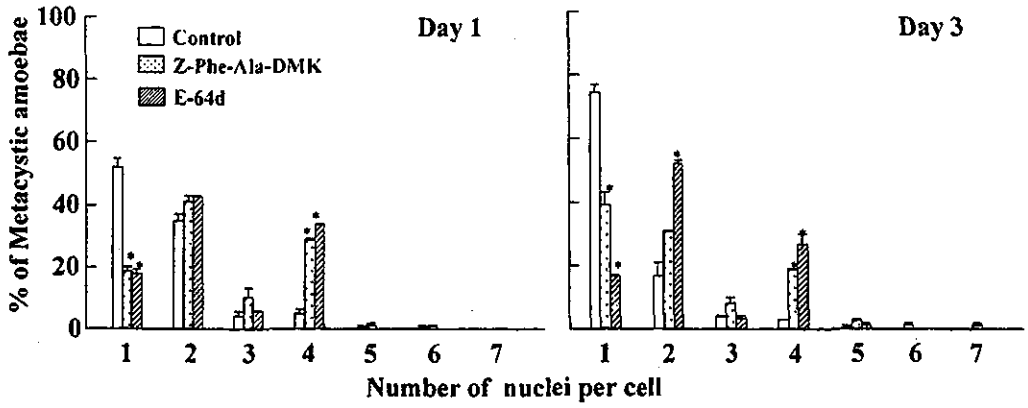

Fig. 3. The effect of cysteine protease inhibitors on the metacystic development of *E. invadens*. The cysts were transferred to a growth medium with or without 100 μM of Z-Phe-Ala-DMK or E-64d. The numbers of nuclei per metacystic amoeba stained with modified Kohn on Days 1 and 3 of incubation were counted, and the percentage of amoebae in each class (1- to 7-nucleate) was determined (each asterisk indicates $P < 0.05$).

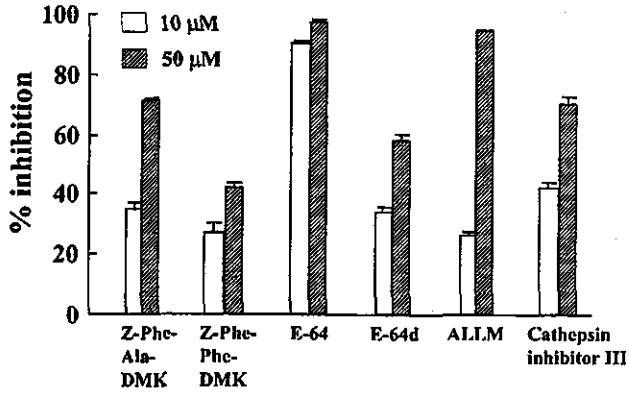

Fig. 4. The effect of cysteine protease inhibitors on cysteine protease activity in the lysates of *E. invadens* cysts. The lysates of *E. invadens* cysts (2×10^7/ml) were incubated with 10 or 50 μM each of the six inhibitors shown in Table 1. The percentages ± SE of inhibition against the control are plotted.

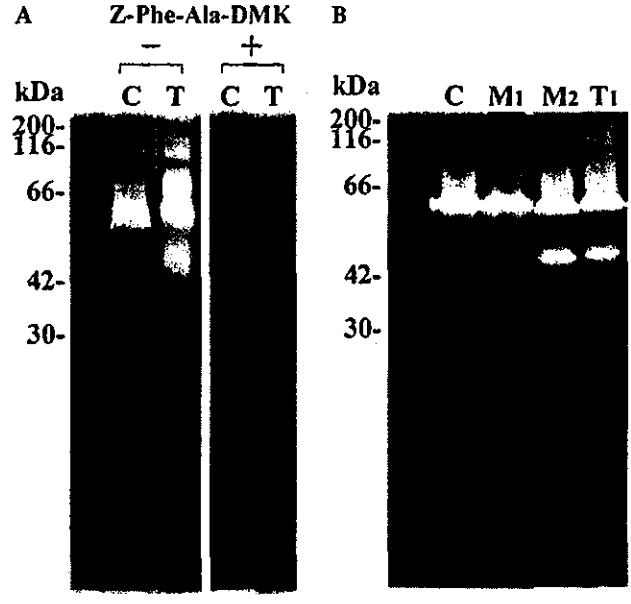

Fig. 5. Gelatin substrate SDS-PAGE of the lysates of *E. invadens* cysts, metacystic amoebae, and trophozoites. (A) Cysts (C); tophozoites (T). Following the removal of SDS, the gels were incubated in buffer alone (–) or with 1 mM Z-Phe-Ala-DMK (+). (B) M1 and M2 were metacystic amoebae from cultures with aphidicolin on Day 1, and those from cultures without the drug on Day 3, respectively. T1 was trophozoites treated similarly as those for metacystic amoebae.

cysteine protease activity in cyst lysates against synthetic peptide substrate Z-Arg-Arg-AMC was inhibited by all of the inhibitors, although there was a difference in their potency.

As shown in Fig. 5A, gelatin substrate SDS-PAGE indicated a major band of 56 kDa, broad bands of 58–66 kDa and 44–54 kDa, and a minor band of 43 kDa in cyst lysates (C). The 56 kDa band and these broad bands detected in cysts were also seen in trophozoite lysates (T). Additional broad bands of 29–41 kDa were also detected in the trophozoite lysates, suggesting a qualitative difference between these two forms. Most of these bands disappeared in the presence of Z-Phe-Ala-DMK. Newly hatched metacystic amoebae with four nuclei (M1) showed a band pattern similar to that of cysts, while more developed metacystic amoebae with one nucleus (M2) showed a band pattern similar to that of trophozoites (T1) (Fig. 5B).

4. Discussion

These results strongly suggest the participation of cysteine proteases in the excystation and metacystic development of *E. invadens*. As cyst viability was not affected by the two cysteine protease inhibitors, Z-Phe-Ala-DMK and E-64d, reduced excystation cannot be due to their toxic effect on cysts. Since other cysteine protease inhibitors used in the present study inhibited cysteine protease activity in cyst lysates, their failure to block

excystation must be due to their lower cell permeability. This is true for E-64, which had a strong inhibitory potency on the cysteine protease activity in cyst lysates. On the other hand, its inhibitory effect on excystation was much lower than E-64d, which is a membrane-permeable synthetic analog of E-64. The process of excystation includes the loosening and separation of amoeba from the cyst wall; the amoeba begins to move about within the cyst. The amoeba then flows back and forth through a small pore in the cyst wall and escapes from the cyst. Thus, cyst wall destruction is necessary for minute perforation of the cyst wall. Since the *Entamoeba* cyst wall contains a mix of protein and chitin (Arroyo-Begovich and Carbez-Trejo, 1982; Frisardi et al., 2000), it is conceivable that both protease and chitinase are essential for cyst wall destruction in the excystation process. The walls of *E. invadens* cysts are electron dense and have a uniform thickness of ~100 nm when observed by electron microscopy (Frisardi et al., 2000). Electron-dense materials were also present in the secretory vesicles and along the plasma membrane. Furthermore, the formation of a crescent-shaped space between the plasma membrane and the cyst wall was observed, and, frequently, some electron-dense bodies projected towards this newly formed space (Chavez-Munguia et al., 2003). Metacysts that endocytose the cyst wall residues were also observed. These observations suggest that secretory vesicles, including proteases and chitinase, are sent in close apposition to the plasma membrane. These enzymes are then secreted into the space between the plasma membrane and the cyst wall to destroy the cyst wall.

The hatched 4-nucleate metacystic amoeba grows rapidly and divides to form eight amoebulae. The results indicate that cysteine proteases are also involved in this metacystic development because the percentage of 4-nucleate amoebae was higher than in the controls on Day 3 of incubation. The results indicate the difference in the band pattern of protease activity between cysts and trophozoites, also changing the band pattern form from cyst-type to trophozoite-type during metacystic development. This is related to our previous results that suggest change in the expression of proteins during metacystic development (Makioka et al., 2003).

Regarding other proteases, we have previously demonstrated that lactacystin, a specific inhibitor of proteasome, had little effect on the excystation and metacystic development of *E. invadens*, suggesting the little contribution of proteasome to these processes (Makioka et al., 2002), although lactacystin inhibited the encystation in vitro of *E. invadens* (Gonzalez et al., 1999; Makioka et al., 2002).

It has recently been demonstrated that *E. histolytica* contains 20 cysteine protease (CP) genes, of which only a small subset is expressed during in vitro cultivation (Bruchhaus et al., 2003). Therefore, it is likely that at least some of these enzymes are required to infect the human host and/or complete the parasite life cycle (Bruchhaus et al., 2003). The gene that encodes CP5 is missing in the closely related but non-pathogenic *E. dispar*, suggesting the potential role of CP5 in the host tissue destruction of *E. histolytica*. Since cyst wall destruction is necessary for excystation by both amoebae, it appears that CP5 is not responsible for cyst wall destruction in either *E. histolytica* or *E. dispar*, or that other CP isoforms are used for it in *E. dispar*. Regarding CP genes in *E. invadens*, it has recently been demonstrated that among the 20 CP genes of *E. histolytica*, 14 homologous genes are found in this parasite (Wang et al., 2003).

Future study will focus on the identification and characterization of CP isoforms responsible for the excystation and metacystic development of *Entamoeba*, which will lead to a more accurate understanding of these processes and also to the identification of targets for vaccination and chemotherapy to inhibit *Entamoeba* infection.

Acknowledgments

We thank Dr. N. Watanabe for his valuable discussion with us, Dr. L. S. Diamond for supplying the *E. invadens*, and T. Yamashita and T. Tadano for their technical assistance. This work was supported by a Grant-in-Aid for Scientific Research from the Ministry of Education, Culture, Sports, and Technology of Japan, and by a Health Science Research Grant for Research on Emerging and Re-emerging Infectious Diseases from the Ministry of Health, Labor, and Welfare of Japan.

References

Arroyo-Begovich, A., Carbez-Trejo, A., 1982. Location of chitin in the cyst wall of *Entamoeba invadens* with the colloidal gold tracers. Journal of Parasitology 68, 253–258.

Bruchhaus, I., Loftus, B.J., Hall, N., Tannich, E., 2003. The intestinal protozoan parasite *Entamoeba histolytica* contains 20 cysteine protease genes, of which only a small subset is expressed during in vitro cultivation. Eukaryotic Cell 2, 501–509.

Chavez-Munguia, B., Cristobal-Ramos, A.R., Gonzalez-Robles, A., Tsutsumi, V., Martinez-Palomo, A., 2003. Ultrastructural study of *Entamoeba invadens* encystation and excystation. Journal of Submicroscopy and Cytological Pathology 35, 235–243.

Cleveland, L.R., Sanders, E.P., 1930. Encystation, multiple fission without encystment, excystation, metacystic development, and variation in a pure line and nine strains of *Entamoeba histolytica*. Archiv für Protistenkunde 70, 223–266.

Diamond, L.S., Harlow, D.R., Cunnick, C.C., 1978. A new medium for the axenic cultivation of *Entamoeba histolytica* and other *Entamoeba*. Transactions of the Royal Society of Tropical Medicine and Hygiene 72, 431–432.

Dobell, C., 1928. Researches on the intestinal protozoa of monkeys and man. Parasitology 20, 357–412.

Eichinger, D., 1997. Encystation of entamoeba parasites. Bioessays 19, 633–639.

Frisardi, M., Ghosh, S.K., Field, J., Van Dellen, K., Rogers, R., Robbins, P., Samuelson, J., 2000. The most abundant glycoprotein of amebic cyst walls (Jacob) is a lectin with five cys-rich, chitin-binding domains. Infection and Immunity 68, 4217–4224.

Garcia-Zapien, A.G., Hernandez-Gutierrez, R., Mora-Galindo, J., 1995. Simultaneous growth and mass encystation of *Entamoeba invadens* under axenic conditions. Archives of Medical Research 26, 257–262.

Geiman, Q.M., Ratcliffe, H.L., 1936. Morphology and life-cycle of an amoeba producing amoebiasis in reptiles. Parasitology 28, 208–230.

Gonzalez, J., Bai, G., Frevert, U., Corey, E.J., Eichinger, D., 1999. Proteasome-dependent cyst formation and stage-specific ubiquitin mRNA accumulation in *Entamoeba invadens*. European Journal of Biochemistry 264, 897–904.

Keene, W.E., Petitt, M.G., Allen, S., McKerrow, J.H., 1986. The major neutral proteinase of *Entamoeba histolytica*. Journal of Experimental Medicine 163, 536–549.

Kumagai, M., Kobayashi, S., Okita, T., Ohtomo, H., 2001. Modifications of Kohn's chlorazol black E staining and Wheatley's trichrome staining for temporary wet mount and permanent preparation of *Entamoeba histolytica*. Journal of Parasitology 87, 701–704.

Laemmli, U.K., 1970. Cleavage of structural proteins during the assembly of the head of bacteriophage T4. Nature 227, 681–685.

López-Romero, E., Villagómez-Castro, J.C., 1993. Encystation in *Entamoeba invadens*. Parasitology Today 9, 225–227.

Makioka, A., Kumagai, M., Ohtomo, H., Kobayashi, S., Takeuchi, T., 2002. Effect of proteasome inhibitors on the growth, encystation, and excystation of *Entamoeba histolytica* and *Entamoeba invadens*. Parasitology Research 88, 454–459.

Makioka, A., Kumagai, M., Kobayashi, S., Takeuchi, T., 2003. *Entamoeba invadens*: inhibition of excystation and metacystic development by aphidicolin. Experimental Parasitology 103, 61–67.

McConnachie, E.W., 1955. Studies on *Entamoeba invadens* Rodhain, 1934, in vitro, and its relationship to some other species of *Entamoeba*. Parasitology 45, 452–481.

McKerrow, J.H., 1989. Parasite proteases. Experimental Parasitology 68, 111–115.

Que, X., Reed, S.L., 2000. Cysteine proteinases and the pathogenesis of amebiasis. Clinical Microbiology Review 13, 196–206.

Rengpien, S., Bailey, G.B., 1975. Differentiation of *Entamoeba*: a new medium and optimal conditions for axenic encystation of *E. invadens*. Journal of Parasitology 61, 24–30.

Rosenthal, P.J., 1999. Proteases of protozoan parasites. Advanced Parasitology 43, 106–139.

Sajid, M., McKerrow, J.H., 2002. Cysteine proteases of parasitic organisms. Molecular and Biochemical Parasitology 120, 1–21.

Sanchez, L., Enea, V., Eichinger, D., 1994. Identification of a developmentally regulated transcript expressed during encystation of *Entamoeba invadens*. Molecular and Biochemical Parasitology 67, 125–135.

Sharma, M., Hirata, K., Herdman, S., Reed, S., 1996. *Entamoeba invadens*: characterization of cysteine proteinases. Experimental Parasitology 84, 84–91.

Shaw, M.K., Roos, D.S., Tilney, L.G., 2002. Cysteine and serine protease inhibitors block intracellular development and disrupt the secretary pathway of *Toxoplasma gondii*. Microbes and Infection 4, 119–132.

Wang, Z., Samuelson, J., Clark, C.G., Eichinger, D., Paul, J., Dellen, K.V., Hall, N., Anderson, I., Loftus, B., 2003. Gene discovery in the *Entamoeba invadens* genome. Molecular and Biochemical Parasitology 129, 23–31.

THE JOURNAL OF BIOLOGICAL CHEMISTRY
Vol. 279, No. 16, Issue of April 16, pp. 16863–16874, 2004
Printed in U.S.A.

An Intestinal Parasitic Protist, *Entamoeba histolytica*, Possesses a Non-redundant Nitrogen Fixation-like System for Iron-Sulfur Cluster Assembly under Anaerobic Conditions*

Received for publication, December 5, 2003, and in revised form, January 21, 2004
Published, JBC Papers in Press, February 2, 2004, DOI 10.1074/jbc.M313314200

Vahab Ali‡, Yasuo Shigeta‡, Umechiyo Tokumoto§, Yasuhiro Takahashi§, and Tomoyoshi Nozaki‡¶‖

From the ‡Department of Parasitology, National Institute of Infectious Diseases, Tokyo 162-8640, the §Department of Biology, Graduate School of Science, Osaka University, Osaka 560-0043, and the ¶Precursory Research for Embryonic Science and Technology, Japan Science and Technology Agency, Tokyo 190-0012, Japan

We have characterized the iron-sulfur (Fe-S) cluster formation in an anaerobic amitochondrial protozoan parasite, *Entamoeba histolytica*, in which Fe-S proteins play an important role in energy metabolism and electron transfer. A genomewide search showed that *E. histolytica* apparently possesses a simplified and non-redundant NIF (nitrogen fixation)-like system for the Fe-S cluster formation, composed of only a catalytic component, NifS, and a scaffold component, NifU. Amino acid alignment and phylogenetic analyses revealed that both amebic NifS and NifU (EhNifS and EhNifU, respectively) showed a close kinship to orthologs from ε-proteobacteria, suggesting that both of these genes were likely transferred by lateral gene transfer from an ancestor of ε-proteobacteria to *E. histolytica*. The EhNifS protein expressed in *E. coli* was present as a homodimer, showing cysteine desulfurase activity with a very basic optimum pH compared with NifS from other organisms. EhNifU protein existed as a tetramer and contained one stable $[2Fe\text{-}2S]^{2+}$ cluster per *monomer*, revealed by spectroscopic and iron analyses. Fractionation of the whole parasite lysate by anion exchange chromatography revealed three major cysteine desulfurase activities, one of which corresponded to the EhNifS protein, verified by immunoblot analysis using the specific EhNifS antibody; the other two peaks corresponded to methionine γ-lyase and cysteine synthase. Finally, ectopic expression of the *EhNifS* and *EhNifU* genes successfully complemented, under anaerobic but not aerobic conditions, the growth defect of an *Escherichia coli* strain, *in* which both the *isc* and *suf* operons were deleted, suggesting that EhNifS and EhNifU are necessary and sufficient for Fe-S clusters of non-nitrogenase Fe-S proteins to form under anaerobic conditions. This is the first demonstration of the presence and biological significance of the NIF-like system in eukaryotes.

Iron-sulfur (Fe-S)[1] clusters are cofactors of proteins probably present in all living organisms. The Fe-S clusters play various important roles in electron transfer, redox regulation, nitrogen fixation, and sensing for regulatory processes (1). Despite the importance of Fe-S proteins, little is known about the biochemical mechanisms of Fe-S cluster assembly *in vivo*. Recent studies using genetic and biochemical methods have unveiled the complex mechanism of the assembly *in vitro* and *in vivo* (2–8). These studies led to the identification of three distinct systems, namely nitrogen fixation (NIF), iron-sulfur cluster (ISC), and mobilization of sulfur (SUF). Two to six components have been shown to participate in the formation of Fe-S clusters, depending upon the system. For instance, in the NIF system, two genes (*nifS* and *nifU*) and their encoded proteins have been shown to be involved in the assembly of Fe-S clusters of the nitrogenase proteins in *Azotobacter vinelandii* (2, 3). NifS is a homodimer of two identical subunits of a pyridoxal-5′-phosphate (PLP)-dependent cysteine desulfurase, which catalyzes the formation of L-alanine and elemental sulfur from L-cysteine. The catalysis is initiated by the formation of a Schiff base between the amino group of cysteine and PLP cofactor (3) and nucleophilic attack of the reactive cysteine by a conserved histidine residue near the active site (9), which in turn mobilizes elemental sulfur. NifU is a scaffold protein for the transient assembly of Fe-S clusters, which are transferred to target apoproteins (10). The NifU protein possesses two distinct types of iron-binding sites (10). One of these binding sites, located in the central third of the NifU protein, binds a stable permanent $[2Fe\text{-}2S]^{2+}$ cluster per subunit as shown in *A. vinelandii* (11). The second type of site, located within the amino-terminal third of the NifU protein, binds a labile mononuclear iron and/or labile cluster (11). Site-directed mutagenesis of the cluster-ligated cysteine residues of NifU from *A. vinelandii* has shown that the permanent $[2Fe\text{-}2S]^{2+}$ clusters play an essential role in the maturation of nitrogenase (12). The NIF system has been identified in only nitrogen-fixing bacteria and non-diazotrophic ε-proteobacteria including *Campylobacter jejuni* and *Helicobacter pylori*, and appears to be involved in Fe-S

* This work was supported by a grant for Precursory Research for Embryonic Science and Technology, Japan Science and Technology Agency (to T. N.), Fellowship PB01155 from the Japan Society for the Promotion of Science (to V. A.), a grant for research on emerging and re-emerging infectious diseases from the Ministry of Health, Labour and Welfare of Japan (to T. N.), and Grants-in-aid 15019120 and 15590378 for Scientific Research on Priority Areas from the Ministry of Education, Culture, Sports, Science and Technology of Japan (to T. N.). The costs of publication of this article were defrayed in part by the payment of page charges. This article must therefore be hereby marked "*advertisement*" in accordance with 18 U.S.C. Section 1734 solely to indicate this fact.

The nucleotide sequence(s) reported in this paper has been submitted to the GenBank™/EBI Data Bank with accession number(s) AB112427.

‖ To whom correspondence should be addressed: Dept. of Parasitology, National Institute of Infectious Diseases, 1-23-1 Toyama, Shinjuku-ku, Tokyo 162-8640, Japan. Tel.: 81-3-5285-1111, extension 2733; Fax: 81-3-5285-1173; E-mail: nozaki@nih.go.jp.

[1] The abbreviations used are: Fe-S, iron-sulfur; NIF, nitrogen fixation; ISC, iron-sulfur cluster; SUF, mobilization of sulfur; PLP, pyridoxal-5′-phosphate; ORF, open reading frame; rEhNifS, recombinant EhNifS; rEhNifU, recombinant EhNifU; DTT, dithiothreitol; GST, glutathione *S*-transferase; CS, cysteine synthase; MGL, methionine γ-lyase.

assembly of the nitrogenase proteins in bacteria that belong to the former group and of non-nitrogenase Fe-S proteins in the latter (13). In contrast to the NIF system, the ISC system is well conserved from bacteria to a wide range of eukaryotes including *Saccharomyces, Arabidopsis, Caenorhabditis, Drosophila,* and *Homo,* and thus, assumed to play more general housekeeping roles for Fe-S cluster assembly. The components of the ISC system are more complex than those of the NIF system: at least six proteins, encoded in a single operon (*iscSUA-hscBA-fdx*) in prokaryotes, *e.g. Escherichia coli*, are involved in the process (4, 6, 7, 14–16). IscS bears sequence identity with NifS and shares function as cysteine desulfurase. IscU is similar to the amino-terminal domain of NifU and shares function as a scaffold for intermediate Fe-S clusters. IscA is closely related to its NIF counterpart (^{Nif}IscA) and responsible for binding labile Fe-S clusters (5, 17) and its transfer to apoproteins (18). HscA and HscB are chaperones that belong to the DnaK and DnaJ proteins families, respectively; but their roles in Fe-S cluster biogenesis remain unclear (19). Protein-protein interaction between each of the components of the ISC system has also been demonstrated (18, 20). The SUF system, a third bacterial system for the assembly of Fe-S clusters, is encoded in the *suf* operon (*sufABCDSE*) and widely present in Eubacteria, Archaea, and plastids (8). Disruption of the *E. coli suf* operon alone did not cause any major defect, whereas lethality was observed when both the *isc* and *suf* operons were inactivated (8). It has also been shown that the SUF system plays a role for Fe-S cluster assembly and/or repair under oxidative stress conditions (21, 22) and iron starvation (23). In addition, the SUF system has been shown to be necessary for virulence of Gram-negative bacterium *Erwinia chrysanthemi,* causing soft-rot disease in plants (21, 24). In addition to the catalytic component SufS, the SUF system requires at least five additional proteins including SufA, a scaffold component, SufC, an unorthodox ATPase of the ABC superfamily, SufB and SufD, which are associated with SufC (24), and SufE, which interacts with SufS and stimulates its cysteine desulfurase activity (25).

Recent studies have demonstrated that a mitochondrial IscS homolog in yeasts (Nfs1) is involved in Fe-S assembly of aconitase and succinate dehydrogenase and thus is essential for mitochondrial function (26). IscS homologs are produced in the cytosol and transported to mitochondria (27) and the nucleus in yeasts and mammals (28, 29). An independent study also revealed that mitochondria play a crucial role in the cluster formation of extramitochondrial Fe-S proteins (30). Thus, the assembly of Fe-S clusters is more complex in eukaryotes than prokaryotes and apparently occurs in mitochondria, cytoplasm, and nucleus, suggesting organelle-specific Fe-S cluster assembly in eukaryotes (31, 32). Thus, the presence or absence, *i.e.* ubiquity and specificity, of these three distinct systems for Fe-S assembly among organisms, together with their specific function in each organism, remains largely unknown, especially in parasitic protozoa.

IscS has been demonstrated in an aerobic protozoan parasite, *Plasmodium falciparum* (33), and two anaerobic protozoa, *Giardia lamblia* and *Trichomonas vaginalis* (34). The latter two parasites belong, together with another enteric parasitic protist *Entamoeba histolytica*, to a group of amitochondrial eukaryotes. Amitochondrial eukaryotes can be divided into two metabolic types (35). Type I organisms including *G. lamblia* and *Entamoeba* lack organelles involved in core energy metabolism. Instead, Fe-S protein (*i.e.* pyruvate:ferredoxin oxidoreductase)-mediated metabolism of pyruvate, substrate-level phosphorylation, and ATP synthesis takes place in the cytosol. In contrast, type II organisms including *Trichomonas,* some ciliates, and chytrid fungi harbor a double-membrane limited organelle, hydrogenosome, which represents a site of the above-mentioned core energy metabolism. The fact that the scaffold component IscU is also present in *Trichomonas* and *Giardia* (36) supported the premise that the machinery for Fe-S cluster assembly in these amitochondrial anaerobic protists shares common features with the ISC system in other organisms. In contrast, the machinery for the Fe-S cluster assembly in *E. histolytica* is largely unknown. The present study demonstrates that *E. histolytica* possesses the NIF-like system as a sole pathway for the biosynthesis of Fe-S clusters. We describe here for the first time the molecular identification of NifS and NifU from *E. histolytica* and provide evidence for the possible horizontal transfer of these genes from an ancestor of ϵ-proteobacteria. We also show biochemical properties distinct from those of other organisms including bacteria and mammals. In addition, we demonstrate that the amebic NifS and NifU are necessary and sufficient for the Fe-S cluster formation under anaerobic conditions by heterologous complementation of an *isc/suf*-lacking mutant of *E. coli*.

EXPERIMENTAL PROCEDURES

Chemicals and Reagents—All chemicals of analytical grade were purchased from Wako (Tokyo, Japan) unless stated otherwise. L-cysteine, L-cystine, *O*-acetyl serine, *N*-acetyl cysteine, DL-homocysteine, D-cysteine, sodium sulfide, *O*-phenanthroline, hydroxylamine, *N,N*-dimethyl-*p*-phenylenediamine sulfate, ferrous ammonium sulfate, PLP, 2-(*N*-morpholino) ethanesulfonic acid, HEPES, *N*-[tris(hydroxymethyl-)methyl]-3-aminopropanesulfonic acid, 3-(cyclohexylamino)-1-propanesulfonic acid, ampicillin, and carbenicillin disodium salt were purchased from Sigma-Aldrich.

Microorganisms and Cultivation—Trophozoites of *E. histolytica* strain HM-1:IMSS cl-6 (37) were maintained axenically in Diamond's BI-S-33 medium (38) at 35.5 °C. Trophozoites were harvested in the late-logarithmic growth phase 2–3 days after inoculation of 1/12 to 1/6 of the total culture volume and washed twice with ice-cold phosphate-buffered saline, pH 7.4, at 4 °C. *E. coli* strains BL21 (DE3) and DH5α were purchased from Novagen (Madison, WI) and Invitrogen, respectively.

Search of the E. histolytica Genome Database—The *E. histolytica* genome databases (contigs and singletons) at The Institute for Genomic Research[2] and Sanger Institute[3] were searched using the TBLASTN algorithm with protein sequences corresponding to the catalytic component of Fe-S cluster formation (NifS, IscS, and SufS) from a variety of species. We also searched for homologs of the Nif- or Isc-specific scaffold component (NifU or IscU, respectively) from *A. vinelandii* and *H. pylori* and components shared by both the Isc and Suf systems (IscA and SufA) of *E. coli, A. vinelandii,* and *P. falciparum,* or components unique to the Suf system (SufB, C, D, and E) from *E. coli, Bacillus subtilis, Methanococcus jannashii, Mycobacterium tuberculosis,* and *P. falciparum.*

Amino Acid Alignments and Phylogenetic Analysis—The sequences of NifS, IscS, NifU, IscU, and related proteins showing similarity in amino acid sequence to EhNifS and EhNifU were obtained from the National Center for Biotechnology Information[4] using the BLASTP search. Alignment and phylogenetic analysis were performed with CLUSTAL W version 1.81 (39) using the neighbor-joining method with the Blosum matrix. A rooted or an unrooted neighbor-joining tree composed of the amino acid sequences of 25 NifS/IscS or 20 NifU/IscU from various organisms was constructed using 352 or 120 shared amino acid positions, respectively, after removing gaps. The most distal members of NifS/IscS that belong to group II including *E. coli* cysteine sulfinate desulfinase (CsdA) and SufS (also known as CsdB or selenocysteine lyase) were used as the out-group to obtain a rooted tree. Trees were drawn by Tree ViewPPC ver.1.6.6 (40). Branch lengths and bootstrap values (1000 replicates) were derived from the neighbor-joining analysis.

Cloning of E. histolytica NifS and NifU—On the basis of the nucleotide sequences of the protein-encoding region of the putative amebic *nifS* and *nifU* genes (*EhNifS* and *EhNifU*) in the genome database, two sets of primers, shown below, were designed to amplify the open reading frames (ORFs) using a cDNA library (41) as a template to construct plasmids to produce EhNifS and EhNifU fusion proteins with a histi-

[2] Internet address: www.tigr.org/tdb/.
[3] Internet address: www.sanger.ac.uk/Projects/E_histolytica/.
[4] Internet address: www.ncbi.nih.gov/.

dine tag or glutathione *S*-transferase at the amino terminus, respectively. The *EhNifS* ORF was amplified with a sense (5′-CCTGGATCC-*GATG*CAAAGTACAAAATCAGT-3′) and an antisense (5′-CCAGGATC-*CTTA*AGCATATGTTGATGATAATTGTC-3′) primer, where BamHI sites are underlined and the translation initiation and termination codons are italicized. The initial step, denaturation at 94 °C for 2 min with platinum *pfx* DNA polymerase (Invitrogen), was followed by the 30 cycles of denaturation at 94 °C for 15 s, annealing at 55 °C for 30 s, and elongation at 68 °C for 2 min, and a final extension for 10 min at 68 °C. The ~1.2-kb PCR fragment was digested with BamHI, electrophoresed, purified with Geneclean kit II (BIO 101, Vista, CA), and cloned into BamHI-digested pET-15b (Novagen) in the same orientation as the T7 promoter. The *EhNifU* ORF was amplified using a sense (5′-*ATG*TCA-AAGAATAAATTAATTGGTGGAGC-3′) and an antisense (5′-*CTA*ATC-TTTCTTTTTGATATTTAAGGT-3′) primer from a cDNA library (the translation initiation and termination sites are italicized). A PCR fragment containing *EhNifU* was end-blunted and cloned into the EcoRI-digested and end-filled site of pGEX2T (Amersham Biosciences). The final constructs were designated pHisEhNifS and pGSTEhNifU, respectively.

Expression and Purification of Recombinant EhNifS and EhNifU Proteins—To express the recombinant proteins in *E. coli*, pHisEhNifS or pGSTEhNifU was introduced into BL21 (DE3) or DH5α cells, respectively. Expression of the recombinant EhNifS (rEhNifS) and EhNifU (rEhNifU) fusion proteins was induced with 1 mM isopropyl-β-thiogalactoside at 30 °C for 5–6 h. The rEhNifS and EhNifU fusion proteins were purified using a Ni^{2+}-NTA column (Novagen) or glutathione-Sepharose 4B column (Amersham Biosciences), respectively, according to the manufacturer's instructions with a few modifications. The bacterial cells were washed, sonicated in the lysis buffer (50 mM Tris-HCl (pH 8.0), 500 mM NaCl, 5 mM 2-mercaptoethanol, and 10 mM imidazole) containing 0.1% Triton X-100 (v/v), 100 μg/ml of lysozyme, and Complete Mini EDTA free protease inhibitor mixture (Roche, Tokyo, Japan), and centrifuged at 24,000 × *g* for 15 min at 4 °C. The histidine-tagged rEhNifS protein was eluted from the Ni^{2+}-NTA column with 100 mM imidazole in 50 mM Tris-HCl (pH 8.0), 300 mM NaCl, and 0.1% Triton X-100 (v/v) and extensively dialyzed in 50 mM Tris-HCl, 300 mM NaCl (pH 8.0), and 0.1% Triton X-100 (v/v) containing 10% glycerol (v/v) and the protease inhibitors. To obtain the rEhNifU, bacterial cells were lysed in 100 mM sodium phosphate buffer (pH 7.4), 2 mM DTT, 0.1% Triton X-100 (v/v), 1 mM phenylmethylsulfonyl fluoride, and 100 μg/ml of lysozyme. After the GST-EhNifU fusion protein was bound to the glutathione-Sepharose 4B column, the rEhNifU was obtained by digestion of GST-EhNifU fusion proteins with thrombin (Amersham Biosciences) in the column or outside of the column, followed by elution from the column. Thrombin was removed by passing through a HiTrap-benzamidine column (Amersham Biosciences), and rEhNifU was extensively dialyzed at 4 °C with 100 mM sodium phosphate buffer (pH 7.4) containing 2 mM DTT.

The purified rEhNifS and rEhNifU proteins were presumed to contain additional 25 (MGSSHHHHHHSSGLVPRGSHMLEDP) or 5 (GSPGI) amino acids at the amino terminus, respectively. The purified enzymes were stored at − 80 °C with 50% glycerol before use. No decrease in the enzyme activity of rEhNifS was observed under these conditions for at least 3 months. Protein concentrations were determined with the Coomassie Brilliant Blue assay (Nacalai Tesque, Inc., Kyoto, Japan) with bovine serum albumin as the standard.

Enzyme Assays—For the cysteine desulfurase assay, rEhNifS protein was reconstituted with PLP by incubating 1 mg/ml of EhNifS with 0.1 mM PLP for 1 h on ice, followed by dialysis for 5–6 h against 100–200-fold volumes of 50 mM *N*-[tris(hydroxymethyl)methyl]-3-aminopropanesulfonic acid/NaOH (pH 9.0) with two buffer exchanges, as described previously for the *Synechocystis* enzyme (42). The cysteine desulfurase activity of EhNifS was monitored based on the production of sulfide using L-cysteine as the substrate (43). The standard EhNifS reaction was performed in 200 μl of reaction mixture (50 mM 3-(cyclohexylamino)-1-propanesulfonic acid/NaOH buffer (pH 10.0) containing 0.02 mM PLP, 1 mM DTT, 10 mM $MgCl_2$, 0.5 mM substrate (L-cysteine), and appropriate amounts (25–50 μg) of purified EhNifS protein). In experiments to determine pH optima, the following buffers were used: 50 mM 2-(*N*-morpholino)ethanesulfonic acid/NaOH for pH 5.5, 6.0, and 6.5; HEPES/NaOH for pH 7.0, 7.5, and 8.0; *N*-[tris(hydroxymethyl)methyl]-3-aminopropanesulfonic acid/NaOH for pH 8.5 and 9.0; and 3-(cyclohexylamino)-1-propanesulfonic acid for pH 9.7, 10.0, 10.5, and 11.0. The reaction was terminated by adding 20 μl of 20 mM *N,N*-dimethyl-*p*-phenylenediamine sulfate in 7.2 N HCl and 20 μl of 30 mM $FeCl_3$ in 1.2 N HCl. After further incubation in the dark for 30 min, the protein precipitate was removed by centrifugation, and then the absorption at 670 nm (A_{670}) of the supernatant was measured. Na_2S (0–100 μM) was used as the standard. Elemental sulfur (S^0) was measured by the cyanolysis method (2, 44) with minor modifications. The alanine production was monitored by measuring pyruvate formed by deamination of alanine using L-alanine aminotransferase in a coupling reaction as described previously (2). The rEhNifS protein was stable in the presence of 10% glycerol, and 90–95% of the initial activity was retained when stored at 4 or − 20 °C for 24 h. However, it was reduced to 25–35% when stored without any additive at room temperature, 4, or − 20 °C for 24 h.

Iron Assay—The iron content of EhNifU was determined by the *O*-phenanthroline method as described, except that the volume of the reaction mixture was reduced (13). The EhNifU samples were acidified by the addition of 3–5 μl of concentrated HCl and then diluted with buffer or distilled water to 0.2 ml. The mixtures were heated to 80 °C for 10 min and cooled down to room temperature; then 0.6 ml of water, 40 μl of 10% hydroxylamine hydrochloride, and 0.2 ml of 0.1% *O*-phenanthroline were added. The mixtures were further incubated at room temperature for 30 min, and then absorbance at 512 nm (A_{512}) was measured with 0–100 μM of ferrous ammonium sulfate as the standard.

Anion-Exchange Chromatography of the Native and Recombinant EhNifS—Approximately 2 × 10^7 *E. histolytica* trophozoites (250–300 mg) was resuspended in 1.0 ml of 100 mM Tris-HCl (pH 8.0), 1.0 mM EDTA, 2.0 mM DTT, and 15% glycerol containing 10 μg/ml of *trans*-epoxysuccinyl-L-leucylamido-(4-guanidino)butane and the protease inhibitor mixture. After sonication, the lysate was centrifuged at 45,000 × *g* for 15 min at 4 °C, filtered through a 0.45 μm cellulose acetate membrane, and dialyzed with the binding buffer (100 mM Tris-HCl (pH 8.0), 1 mM DTT, 1 mM EDTA, 0.1 mM phenylmethylsulfonyl fluoride, 1 μg/ml of *trans*-epoxysuccinyl-L-leucylamido-(4-guanidino)butane and 10% glycerol) using a Centricon YM-10 (Millipore). The sample (1 ml) containing ~5 mg of soluble lysate protein or recombinant EhNifS was applied to a Mono Q 5/5 HR column preequilibrated with the binding buffer on the AKTA Explorer 10S system (Amersham Biosciences). After the column was extensively washed with the binding buffer, bound proteins were eluted with a linear gradient of 0–0.7 M NaCl. All of the fractions (0.3 ml) were analyzed for cysteine desulfurase activity as described above and subjected to immunoblot analyses as described below.

Size Exclusion Chromatography of the Native and Recombinant EhNifS and EhNifU—Approximately 500 μg of recombinant proteins or the fractions that were eluted from the anion-exchange chromatography were dialyzed against gel filtration buffer (100 mM Tris-HCl (pH 8.0), 0.1 M NaCl) at 4 °C and concentrated to 1 ml with the Centricon YM-10. A Sephacryl S300 HR Hiprep prepacked column (60-cm long and 1.6-cm in diameter) (Amersham Biosciences) was preequilibrated, loaded, and eluted with the gel filtration buffer of a flow rate of 0.5 ml/min. The same column was calibrated with ferritin (440 kDa), catalase (232 kDa), aldolase (158 kDa), albumin (67 kDa), ovalbumin (43 kDa), and chymotrypsinogen A (25 kDa) (Amersham Biosciences).

Immunoblot Analysis—Polyclonal antisera against recombinant EhNifS and EhNifU were raised in rabbits by Kitayama-Rabes (Nagano, Japan). Immunoblot analysis was carried out as described previously (45). Primary antibodies were used at either 1:500 (for anti-EhCS1 antiserum) (41) or 1:1000 (for anti-methionine γ-lyase 2 (EhMGL2) (46) and anti-EhNifS antisera). The blots were visualized using alkaline phosphatase-conjugated anti-rabbit IgG antibody (ICN-Cappel, Cappel, OH) (1:2000) with nitro blue tetrazolium/5-bromo-4-chloro-3-indolyly phosphate solution (Roche) according to the manufacturer's protocol.

Heterologous Expression of the Amebic NifS and NifU Genes in the isc/suf-Mutant E. coli Strain—A plasmid to coexpress EhNifS and EhNifU in *E. coli* was constructed. The EhNifS and EhNifU ORF were PCR-amplified using a sense (5′-CTCTCTAGA*GATG*CAAAGTACAAA-TCAGT-3′) and an antisense (5′-GGTACATGT*TTA*aaactcctcAGCATA-TGTTGATGATAATTGTC-3′) primer (EhNifS); a sense (5′-GCA*CCATGG*CAAAGAATAAATTAATTGGTGGAG-3′) and an antisense (5′-GCTGCTAGC*CTA*ATCTTTCTTTTTGATATTTAAGG-3′) primer (EhNifU), where XbaI, PciI, NcoI, and NheI sites are underlined, the translation initiation and termination codons are italicized, and the ribosome binding sequence is shown in lowercase. Because of the engineered ribosome-binding sequence, the resulting EhNifS protein has three additional amino acids (EEF) at the carboxyl terminus. The PCR fragments of EhNifS and EhNifU were digested with appropriate enzymes and cloned in tandem in the XbaI and NheI double-digested pRKNMC (7) to produce pRKEhNifSU. The pRKISC or pRKSUF, which

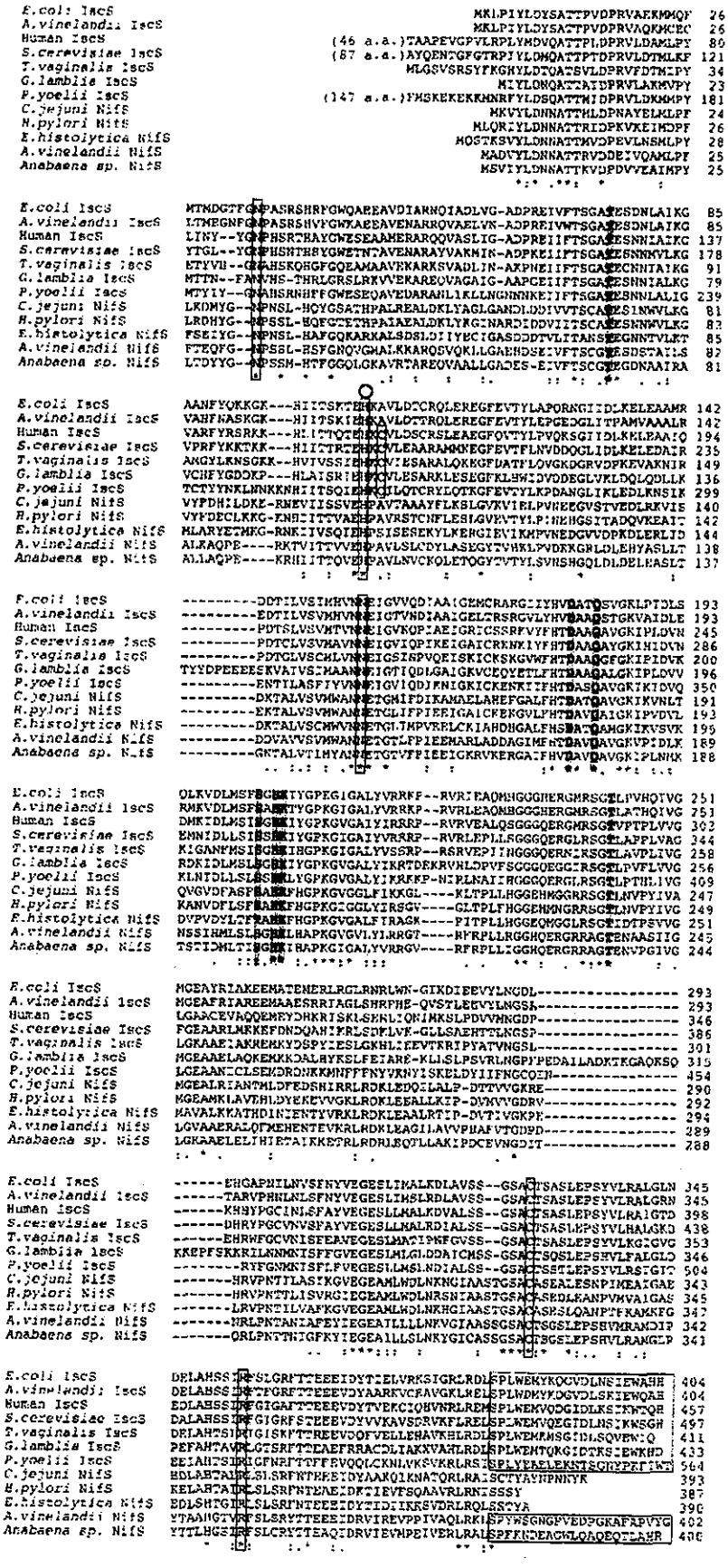

FIG. 1. **Multiple alignment of deduced amino acid sequences of NifS/IscS from *E. histolytica* and other organisms.** Protein sequences were aligned using the CLUSTAL W program (www.ebi.ac.uk/clustalw/). Sequences are as follows: *Escherichia coli* IscS (accession number A65030); *Azotobacter vinelandii* IscS and NifS (AAC24472, P05341); human IscS (AAD09187); *Saccharomyces cerevisiae* IscS (Nfs1p, tRNA splicing protein SPL1 M98808); *Trichomonas vaginalis* IscS (TvIscS-2, AAK69174); *Giardia lamblia IscS* (AAK39427); *Plasmodium yoelii* IscS (EAA21518); *Campylobacter jejuni* NifS (CAB72709); *Helicobacter pylori* NifS (D64547); *E. histolytica* NifS (AB112427); and *Anabaena sp.* PCC 7120 NifS (P12623). Conserved residues involved in PLP binding are *highlighted* with a *gray* background. Invariable cysteine and other residues involved in substrate binding are *boxed* with *thin lines*. A carboxyl-terminal extension consisting of 20–21 amino acids including the consensus sequence SPL(W/Y)(E/D)(M/L)*X*(K/Q)*X*G(I/V)D(L/I)*XX*(/V)*XWXXX* found in proteobacterial and eukaryotic IscS, and a similar extension found in nitrogen-fixing bacteria is also *boxed* with *thin lines*. A *circle* on the alignment (also *boxed*) indicates the conserved histidine involved in the substrate deprotonation. *Asterisks* indicate identical amino acids; *colons* and *dots* indicate conserved amino acid substitutions; and *dashes* indicate computer-generated gaps.

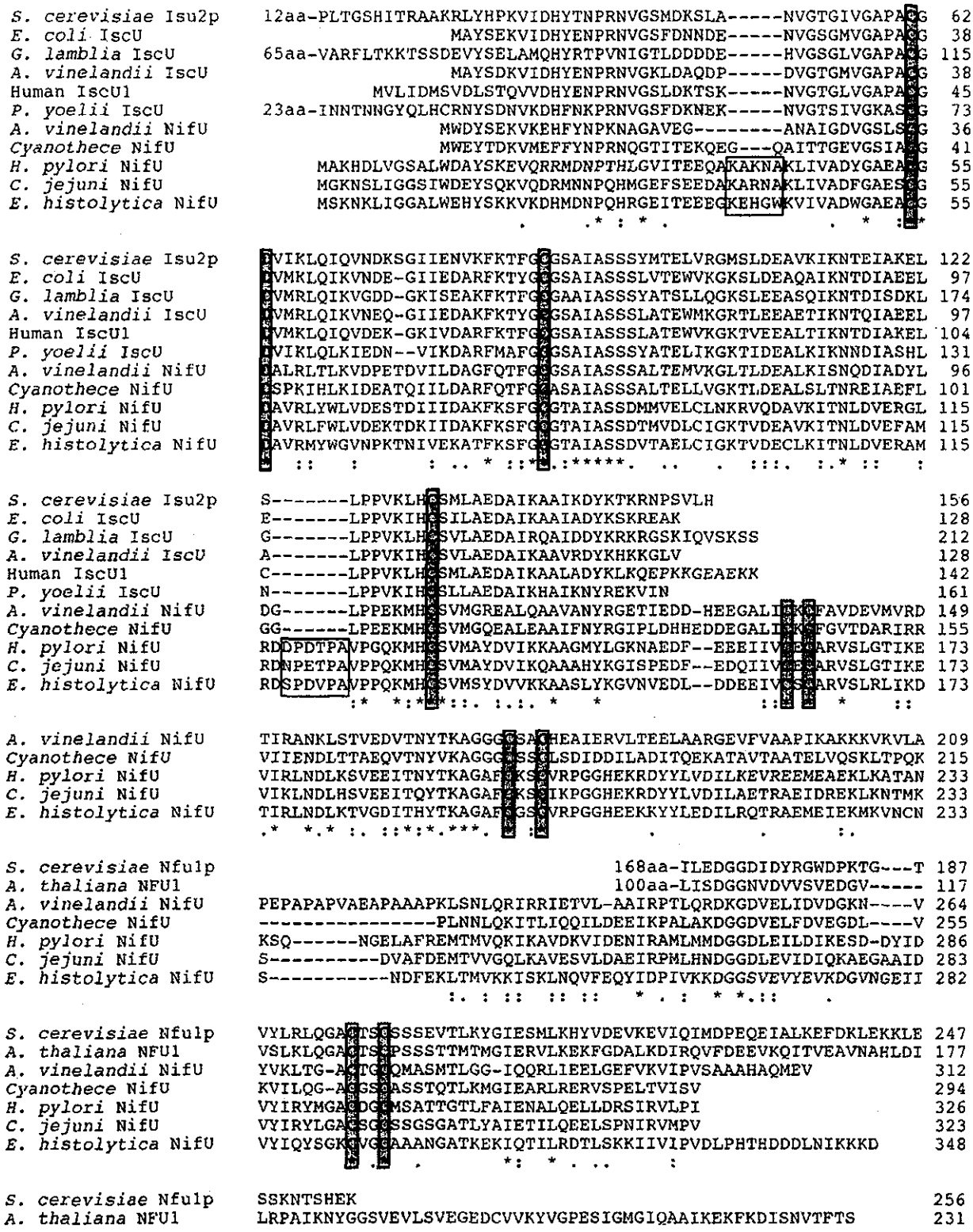

FIG. 2. **Multiple alignment of deduced amino acid sequences of NifU/IscU/Nfu from a variety of organisms including *E. histolytica*.** Protein sequences were aligned using the CLUSTAL W program. Sequences are as follows: *S. cerevisiae* Isu2p (NP_014869); *E. coli* IscU (AP002562.1); *G. lamblia* IscU (EAA38480); *A. vinelandii* IscU and NifU (AAC24473, AAA22167); human IscU1 (AAG37427); *P. yoelii* IscU (EAA18972); *Cyanothece sp.* PCC 8801 NifU (AAC33371.1); *H. pylori* NifU (NP_222928.1); *C. jejuni* NifU (NP_281434.1); and *E. histolytica* NifU (AAK85709). Conserved cysteine and aspartate residues are *boxed* with a *gray* background. Unique insertions shared by NifU from *E. histolytica* and ε-proteobacteria are *boxed*. *Asterisks* indicate identical amino acids; *colons* and *dots* indicate conserved amino acid substitutions; and *dashes* indicate computer-generated gaps.

contains the *E. coli iscSUA-hscBA* or *sufABCDSE* operon in pRKNMC, respectively (6, 8), pRKEhNifSU, or pRKNMC was introduced into *E. coli* strain UT109 [Δ(*iscUA-hscBA*)::Km^r, Δ(*sufABCDSEU*)::Gm^r] harboring pKO3-SUF, a complementation plasmid carrying *E. coli sufABCDSE* and the temperature-sensitive replication origin. The transformants were plated and grown at 30 °C (permissive temperature) and

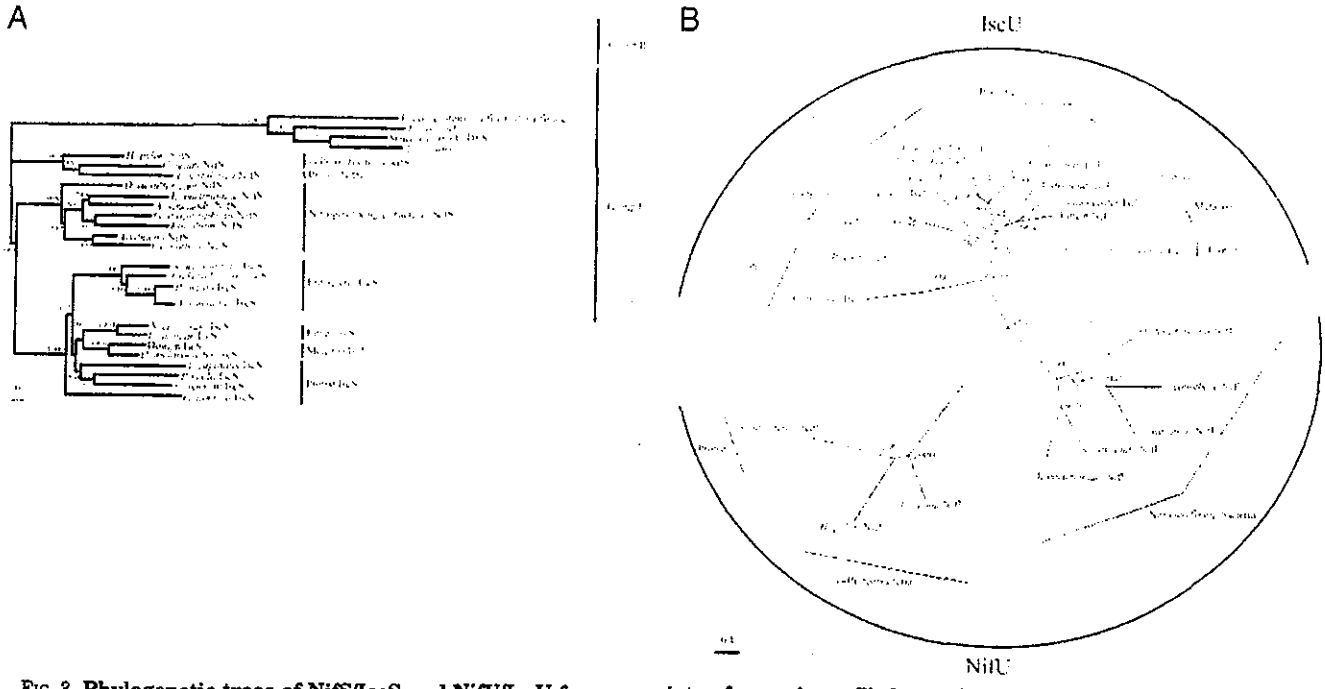

FIG. 3. **Phylogenetic trees of NifS/IscS and NifU/IscU from a variety of organisms.** Phylogenetic reconstructions for NifS/IscS (*A*) and NifU/IscU (*B*) were performed using the CLUSTAL W program, and trees were drawn using the Tree view PPC program. NifS/IscS: *E. coli* (CsdA or cysteine sulfinate desulfinase, F65063 and SufS or CsdB, H64925); *Synechocystis sp.* (S76601); *A. thaliana* (AAF22900); *Desulfovibrio desulfuricans* NifS (ZP_00129032.1); *Klebsiella pneumoniae* NifS (S37296); *Gluconacetobacter diazotrophicus* NifS (CAA31118.1); *Rhizobium sp.* NifS (P55690); *Cyanothece sp.* PCC 8801NifS (AAC33372.1); *Neisseria meningitidis* IscS (Z2491); *Pseudomonas putida* KT2440 (NP_746465); *Candida albicans* IscS (P87187); *Drosophila melanogaster* IscS (AAF53143); *Cryptosporidium parvum* IscS (AAK38323.1). NifU/IscU: *K. pneumoniae* NifU (P05343); *Anabaena variabilis* NifU (AAA93019); *D. desulfuricans* NifU (ZP_00129033); *D. melanogaster* IscU (NP_649840); *A. thaliana* IscU1 (NP_193953); *Pseudomonas putida* KT2440 (NP_746465); *Ralstonia metallidurans* IscU (ZP_00021929); *Vibrio cholerae* IscU (NP_230398); *Neurospora crassa* IscU (CAA04802); *C. parvum* IscU (AAL83713). Also see legends of Figs. 1 and 2 for other proteins. Numbers at the nodes represent bootstrap values for 1000 replicates. The *scale bar* indicates 0.1 substitutions at each amino acid position.

43 °C (restrictive temperature) in Luria broth containing 0.5% D-glucose and 10 μg/ml of tetracycline under ambient atmosphere or in anaerobic culture bags using Anaerocult A (Merck).

RESULTS

Identification and Features of EhNifS and EhNifU Genes and Their Encoded Proteins—We identified putative *NifS/IscS/SufS* and *NifU/IscU* gene homologs in the *E. histolytica* genome database as described in "Experimental Procedures." Putative *EhNifS* and *EhNifU* genes contained an ORF of 1173 and 1047 bp encoding a protein of 390 and 348 amino acids with predicted molecular masses of 42.8 and 38.9 kDa and a pI of 5.9 and 5.6, respectively. Neither the PSORT II program, which predicts protein localization in cells[5] nor a Kite-Doolittle hydropathy plot suggested any possible cellular localization other than a cytosolic distribution for both EhNifS and EhNifU. A protein alignment of 26 NifS/IscS/SufS homologs from Archaea, bacteria, fungi, protists, plants, and metazoa revealed (an alignment of only representative members is shown in Fig. 1) that EhNifS showed greatest homology (52–55% identity) to NifS from ϵ-proteobacteria *Campylobacter jejuni* and *Helicobacter pylori*; 37–42% identity to NifS from nitrogen-fixing Eubacteria including *A. vinelandii, Klebsiella pneumoniae,* and cyanobacteria; and 32–33% identity to IscS from nitrogen-fixing and non-fixing Eubacteria, fungi, and other protists including *G. lamblia, T. vaginalis, P. yoelii,* and *Cryptosporidium parvum,* and metazoa. EhNifS also showed limited homology (21–24% identity) to other (group II) NifS/IscS/SufS homologs including CsdA (cysteine sulfinate desulfinase) and SufS (CsdB or selenocysteine lyase) from *E. coli*, a hypothetical protein from *Synechocystis*, and a chloroplast homolog from *Arabidopsis thaliana* (data not shown; see also "phylogenetic analyses" and Fig. 3*A*). All of the residues of the active site and amino acids implicated in the cysteine desulfurase activity were conserved: (i) His^{106} (numbered according to EhNifS), which is involved in the initial deprotonation of the substrate (9); (ii) the PLP-binding site with the Schiff base-forming amino acids Lys^{208}, Asp^{182}, and Gln^{185} that bind the pyridine nitrogen and the phenolate oxygen of PLP, respectively; (iii) Thr^{76}, His^{207}, Ser/Thr^{205}, and Thr^{243}, involved in the formation of an additional six hydrogen bonds anchoring the phosphate group of PLP (2, 9); and (iv) the substrate-binding site including Cys^{330}, which provides a reactive cysteinyl residue (3), as well as Arg^{356}, Asn^{157}, and Asn^{35}, which anchor the cysteine with a salt bridge and hydrogen bond (9). A carboxyl-terminal extension consisting of 20–21 amino acids including the consensus sequence SPL(W/Y)(E/D)(M/L)*X*(K/Q)*X*G(I/V)D(L/I)*XX*(/V)*X*-W*XXX* was previously proposed to differentiate proteobacterial and eukaryotic IscS from homologs of all other organisms (34) but also is present in nitrogen-fixing bacteria and cyanobacteria (Fig. 1). However, this extension is absent in the NifS homologs from *E. histolytica* and ϵ-proteobacteria.

A protein alignment of 21 NifU/IscU/Nfu1p homologs from Archaea, bacteria, fungi, protists, plants, and metazoa revealed (an alignment of only representative members is shown in Fig. 2) that EhNifU showed, similar to NifS, greatest homology (55–56% identity) to NifU from ϵ-proteobacteria and less homology (32–35% identity) to NifU from diazotrophic Eubacteria throughout the proteins. The amino-terminal half of EhNifU (residues 15–151) also exhibited 28–37% identity to IscU from non-diazotrophic bacteria, fungi, other protists, plants, and metazoa. The amino terminus of EhNifU showed insertions of five and six amino acids at two positions (38–42 and 118–123), which are also observed in ϵ-proteobacteria. In addition, the

[5] Internet address: psort.ims.u-tokyo.ac.jp/.

carboxyl-terminal half of EhNifU (178–348) showed limited homology (12–14% identity) to Nfu1p homologs from *S. cerevisiae* and *A. thaliana*. Nine of 12 cysteine residues of EhNifU (Cys^{54}, Cys^{81}, Cys^{131}, Cys^{161}, Cys^{163}, Cys^{196}, Cys^{199}, Cys^{291}, and Cys^{294}) were conserved. These residues include three cysteines (Cys^{54}, Cys^{81}, and Cys^{131}) in the amino terminus, which constitute a binding site for iron and transient Fe-S cluster (5) and are essential for the function of IscU, Isu1p, and NifU (12, 47). In contrast, Cys^{95} was conserved only in *EhNifU* and among NifU proteins from ϵ-proteobacteria. The central portion of EhNifU contains four conserved cysteine residues, Cys^{161}, Cys^{163}, Cys^{196}, and Cys^{199}, which were shown to be responsible for permanent $[2Fe\text{-}2S]^{2+}$ cluster binding as described in a mutational study on *A. vinelandii* NifU (12). Two additional cysteines (Cys^{291} and Cys^{294}) at the carboxyl-terminal region that are present in mammalian Nfu and have been shown to function as a scaffold protein for one transient $[4Fe\text{-}4S]^{2+}$ cluster per two Nfu monomers (29) are also conserved in EhNifU. Asp^{56} was conserved in all species and was implicated in the release of the NifU-bound transient Fe-S cluster (10).

Phylogenetic Analysis of EhNifS and EhNifU—NifS/IscS/SufS homologs were shown previously to form two distinct groups, I and II (48). Distal members of the homologs that belong to group II (SufS and CsdA) were used as the outgroup to examine the phylogenetic relationship of EhNifS. IscS from a wide range of non-diazotrophic Eubacteria other than ϵ-proteobacteria, fungi, metazoa, and parasitic protists (*G. lamblia*, *T. vaginalis*, *P. yoelii*, and *C. parvum*) and NifS from nitrogen-fixing Eubacteria formed independent clades that were well supported by high bootstrap values (99.8–100%) (Fig. 3*A*). The amebic NifS formed a separate clade (also well supported by a 100% bootstrap value) with ϵ-proteobacteria *H. pylori* and *C. jejuni*. This, together with high amino acid identities among this group, reinforces a close kinship of EhNifS with homologs from ϵ-proteobacteria.

The phylogenetic relationship of EhNifU with 20 other NifU/IscU homologs from Archaea, bacteria, fungi, protists, plants, and metazoa was presented as a radial unrooted tree as an appropriate outgroup was not available (Fig. 3*B*). IscU from nitrogen-fixing and non-fixing bacteria, fungi, protists except for *E. histolytica*, plants, and metazoa and NifU from nitrogen-fixing bacteria, cyanobacteria, ϵ-proteobacteria, and *E. histolytica* form two independent clades, well supported by high bootstrap values (92–96%). *EhNifU showed strong* affinity for homologs from ϵ-proteobacteria as shown in the case of EhNifS and represents an independent group well separated from the group of NifU from nitrogen-fixing bacteria. This, together with the high amino acid identities and common insertions, clearly supported a close association of *E. histolytica* NifU with NifU from ϵ-proteobacteria.

Expression and Purification of rEhNifS and rEhNifU Proteins—The rEhNifS protein was purified at high yield, ~100 mg/l of *E. coli* culture. Cells, cell extracts, and purified EhNifS were yellowish in color. The rEhNifS protein revealed an apparently homogeneous band of 45 kDa on SDS-PAGE (Fig. 4*A*), which was consistent with the predicted size of the deduced EhNifS protein with the extra 25 amino acids added at the amino terminus. The purified rEhNifS protein was evaluated ~98% pure by densitometric measurement of the Coomassie-stained SDS-PAGE gel. The cell pellet of the *E. coli* that overexpressed the GST-EhNifU fusion protein was brown in color. The purified recombinant GST-EhNifU protein also showed a slight brownish color, characteristic of Fe-S proteins. The recombinant GST-EhNifU protein showed an apparently homogeneous band of 65 kDa on SDS-PAGE run under reducing or non-reducing conditions (Fig. 4*B*, data for under the non-reducing conditions not shown), which was consistent with the predicted size of the deduced monomeric EhNifU protein with the extra 26-kDa GST fused at the amino terminus. This also indicates that GST-EhNifU does not form an inter-molecule disulfide bridge. After final purification, rEhNifU protein was evaluated ~98% pure. The final yield of purified rEhNifU was lower than rEhNifS (3 mg/l of *E. coli* culture). The antibody raised against either rEhNifS or rEhNifU recognized an apparently single protein in the *E. histolytica* lysate, which is similar in size to rEhNifS or rEhNifU, respectively (Fig. 4, *A* and *B*, *right panels*), confirming the molecular mass of native *E. histolytica* proteins. We roughly estimated from immunoblots of a series of diluted recombinant proteins that the ameba contains a comparable amount of EhNifS and EhNifU, which consists of ~0.1% of the total soluble protein (data not shown).

Biochemical Characterization of Recombinant EhNifS—The purified rEhNifS protein showed an absorption spectrum typ-

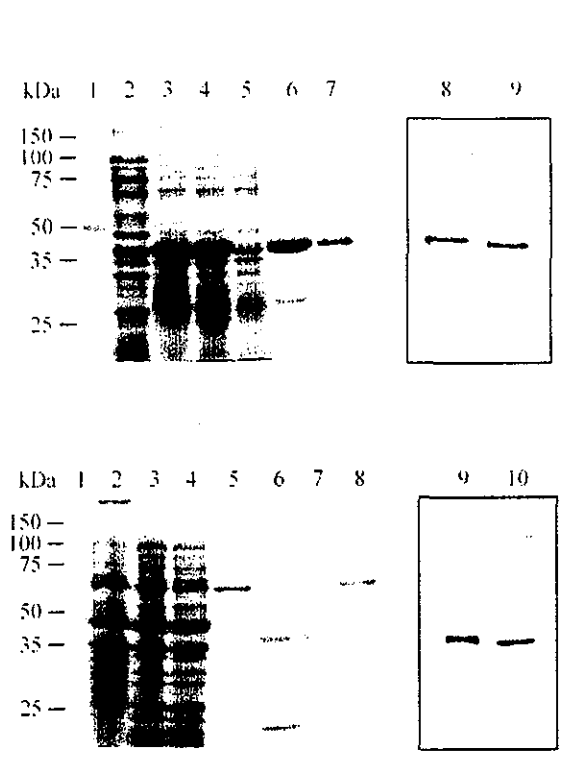

FIG. 4. **Expression and purification of recombinant EhNifS and EhNifU proteins.** *A*, EhNifS was expressed as a protein containing the amino-terminal histidine tag and purified with the Ni^{2+}-NTA column as described in "Experimental Procedures." The total cell lysate and samples at each purification step were electrophoresed on 12% SDS-PAGE gel and stained with Coomassie Brilliant Blue. *Lane 1*, protein marker; *lane 2*, control (an *E. coli* transformant with pET-15b control vector); *lane 3*, total lysate of cells expressing EhNifS; *lane 4*, supernatant of *lane 3* after 24,000 × *g* centrifugation; *lane 5*, unbound fraction of the Ni^{2+}-NTA column of *lane 4*; *lane 6*, elute from the Ni^{2+}-NTA column with 100 mM imidazole; *lane 7*, elute from the gel filtration column. The *right panel* shows a Western blot for EhNifS: *lanes 8* and *9*, 10 ng of rEhNifS protein and 10 μg of soluble *E. histolytica* lysate protein, respectively. *B*, EhNifU was expressed as a GST-fusion protein and purified with a glutathione-Sepharose 4B column. *Lane 1*, protein marker; *lane 2*, total cell lysate of an *E. coli* transformant expressing EhNifU; *lane 3*, supernatant of *lane 2* after 24,000 × *g* centrifugation; *lane 4*, unbound fraction of the glutathione-Sepharose 4B column; *lane 5*, fraction eluted with 10 mM glutathione from the glutathione-Sepharose 4B column; *lane 6*, thrombin-digest of *lane 5*; *lane 7*, purified rEhNifU after the removal of the GST portion; *lane 8*, GST-EhNifU purified by gel filtration chromatography. The *right panel* shows a Western blot for EhNifU: *lanes 9* and *10*, 10 ng of rEhNifU protein and 10 μg of soluble *E. histolytica* lysate protein, respectively.

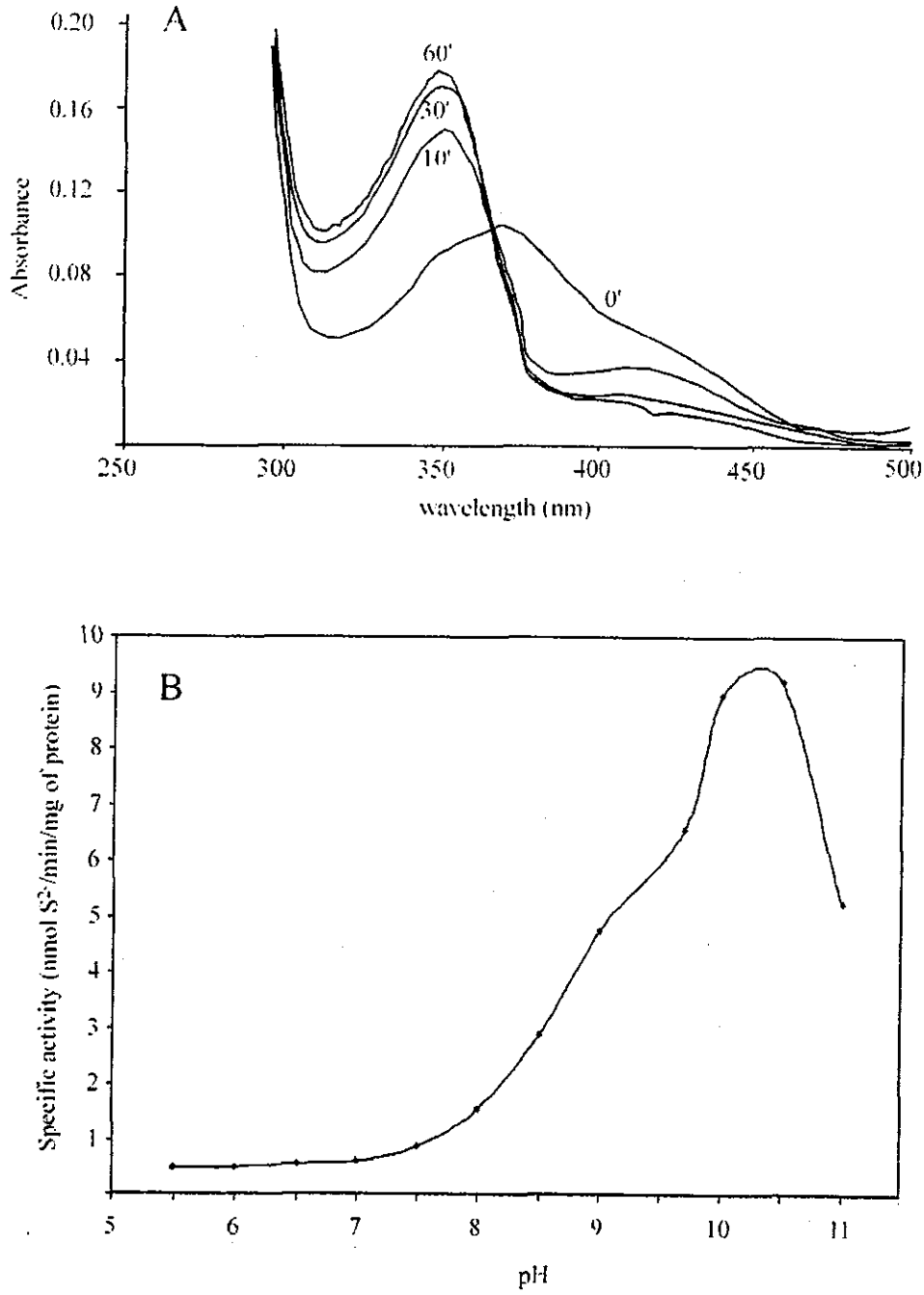

FIG. 5. **UV-visible absorption spectra and pH optimum of EhNifS protein.** *A*, UV-visible spectra of purified EhNifS protein (1 mg/ml) in the absence of cysteine (spectrum 0') and presence of 0.5 mM cysteine (spectra 10, 30, and 60 min) in 0.1 M Tris-HCl buffer, pH 8.0. *B*, the pH effects on cysteine desulfurase activity of rEhNifS was measured in 50 mM buffers containing 0.5 mM L-cysteine, 1 mM DTT, 10 mM $MgCl_2$, 20 μM PLP, and 25 μg of purified protein as described in "Experimental Procedures." Each experiment was carried out at least twice in duplicate.

ical of a PLP-binding protein, a characteristic peak at 370–380 nm (Fig. 5*A*). Incubation with 0.5 mM L-cysteine shifted the peak to 348 nm, with a broad shoulder at 410 nm (Fig. 5*A*), similar to NifS from *H. pylori* (13). In contrast, *A. vinelandii* NifS showed major and minor peaks at 416 and 370 nm, respectively, in the presence of L-cysteine (2). The spectral change was observed previously for NifS-like protein from *T. maritima* and proposed to be attributable to deprotonation/protonation of aldimine, leading to the formation of either germinal diamine or enolimine species (49), which occurs in conjunction with persulfide formation (9). The whole reaction required 10–15 min to complete. At 30 min after the addition of cysteine, no further spectral change was observed. The optimum pH for EhNifS was 10–10.5; the half-maximum activity was reached at about pH 9.0 (Fig. 5*B*). The rEhNifS protein showed cysteine desulfurase activity, as measured in sulfide production, of ~9.5 nmol/min/mg pure protein with 0.5 mM cysteine, which is comparable to NifS from *H. pylori* (9.9 nmol/min/mg with 50 mM cysteine) (13) and lower than other bacterial homologs (*A. vinelandii* NifS, 89.4 nmol/min/mg with 0.5 mM cysteine (2); *A. vinelandii* IscS, 67.6 nmol/min/mg with 2.5 mM cysteine (4); *E. coli* IscS, 78 nmol/min/mg with 2.5 mM cysteine (16); *E. coli* CSD, 3.4 μmol/min/mg (V_{max}) (48); and *E. coli* SufS, 0.019 or 0.9 μmol/min/mg (V_{max}) in the absence or presence of SufE, respectively (25)). Among a variety of possible substrates, EhNifS was shown to be specific for L-cysteine and L-cystine. No

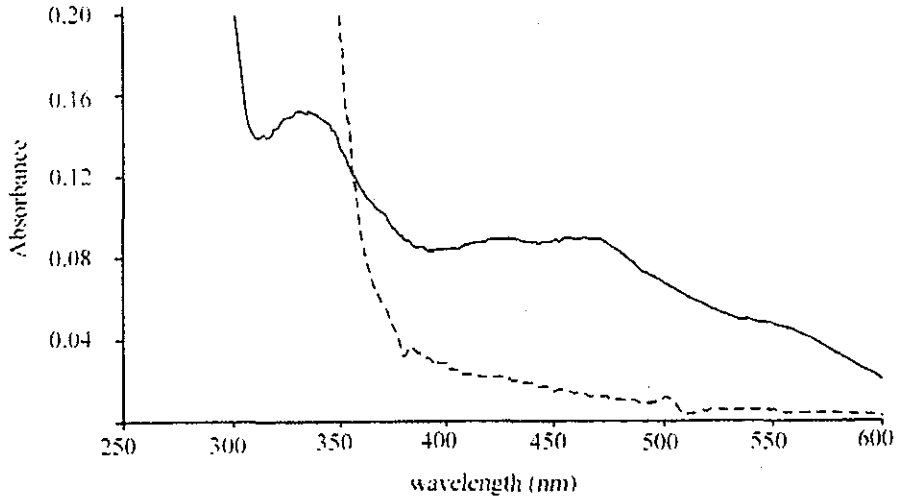

FIG. 6. **Absorption spectrum of EhNifU protein.** UV-visible absorption spectra of EhNifU under non-reducing (as *purified*) (*solid line*) conditions or under sodium dithionite-reducing conditions (*dashed line*) are shown. The protein concentration was 0.8 mg/ml, and the sample was reduced with a 20-fold molar excess of sodium dithionite. The dominant peak at 315 nm in the reduced spectrum (A_{315} = 0.972, not shown) was attributable to dithionite.

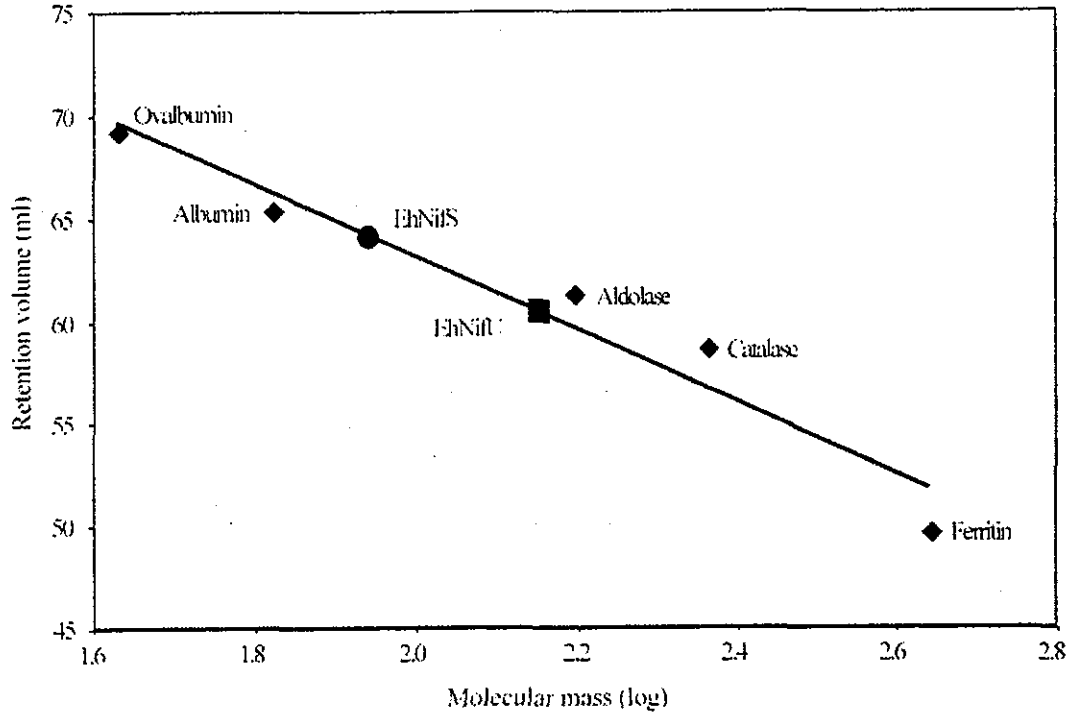

FIG. 7. **Determination of the molecular masses of rEhNifS and rEhNifU proteins.** The molecular masses of rEhNifS and rEhNifU were determined by gel filtration chromatography on a Sephacryl S-300 HR (60 × 1.6-cm) column. The void volume of the column was identified using blue dextran. *Diamonds* represent protein markers: ovalbumin (43 kDa), albumin (67 kDa), aldolase (158 kDa), catalase (232 kDa), and ferritin (440 kDa). *A circle* and a *rectangle* represent rEhNifS and rEhNifU, respectively.

sulfide production was observed when D-cysteine, *N*-acetylcysteine, DL-homocysteine, DL-selenocysteine, cysteine sulfinic acid, or L-cysteic acid was used at up to 5 mM. rEhNifS showed 40–50% cysteine desulfurase activity toward L-cystine (4.0 nmol sulfide/min/mg) in the presence of DTT. Both alanine and cyanolysis assays also showed the comparable cysteine desulfurase activity of rEhNifS (9.1 nmol alanine/min/mg and 8.0 nmol sulfur/min/mg, respectively) with 0.5 mM cysteine, whereas rEhNifS showed the specific activity of 3.0 nmol alanine/min/mg against L-cystine by alanine assay.

Biochemical Characterization of Recombinant EhNifU—Spectrophotometric analysis of the purified recombinant EhNifU revealed peaks at 330, 420, and 460 nm and a shoulder at 550 nm, which indicates the presence of a $[2Fe\text{-}2S]^{2+}$ cluster (Fig. 6), as described for NifU of *A. vinelandii* (11). Extinction coefficients of EhNifU per 38-kDa subunit were also consistent with the premise that EhNifU contains a $[2Fe\text{-}2S]^{2+}$ center: the peaks at 330 nm (extinction coefficient, 11700 M^{-1} cm^{-1}), 420 nm (6800 M^{-1} cm^{-1}), and 460 nm (7000 M^{-1} cm^{-1}), a shoulder at ~550 nm (4700 M^{-1} cm^{-1}), and a ratio between 280 and 335 nm (A_{335}/A_{280}) of 0.27. The dithionite-reduced rEhNifU showed, in contrast, a relatively featureless spectrum, which increased in intensity at shorter wavelengths because of dithionite. Effects of Fe chelators on the cluster structure were assessed by treating oxidized and reduced rEhNifU with a 40-fold excess of 2,2′-dipyridyl or EDTA. No change of A_{520} was observed over 2 h (results not shown), indicating that the Fe-S cluster is either stable or inaccessible to solvent, which is also similar to *A. vinelandii* NifU (11). The iron analysis indicates that EhNifU contains two irons per subunit (2.1 ± 0.084 Fe/subunit from three independent EhNifU preparations).

Determination of Multimeric Structure of EhNifS and EhNifU—The cysteine desulfurase activity of rEhNifS was eluted at the predicted molecular mass of 85–95 kDa (Fig. 7) by gel

filtration chromatography. This is consistent with the notion that rEhNifS exists as a dimer of two identical subunits (42.5 kDa plus 2.6 kDa corresponding to the histidine tag), which is similar to all other organisms reported earlier. EhNifU was eluted at 150–170 kDa; GST-EhNifU was also eluted at 260–280 kDa (Fig. 7). These results show clearly that EhNifU is a tetramer irrespective of the presence or absence of a fusion partner. Elution patterns of EhNifU remained unchanged when EhNifU was pretreated with 2 mM DTT and fractionated in the presence of DTT (results not shown).

Anion-Exchange Chromatographic Separation of Native and Recombinant Cysteine Desulfurase Activity—To correlate native cysteine desulfurase activity in the *E. histolytica* lysate with the recombinant enzyme, the lysate from the trophozoites and rEhNifS were subjected to chromatographic separation on a Mono Q anion exchange column and analyzed by cysteine desulfurase assay and also immunoblotting using anti-EhCS, EhMGL, and EhNifS antibodies. *E. histolytica* trophozoites possess two isotypes of CS (CS1 and CS2) (41) and two isotypes of MGL (MGL1 and MGL2) (46), both of which showed substantial cysteine desulfurase activity.[6] Thus, we attempted to separate native NifS from the CS and MGL isotypes. The *E. histolytica* lysate showed three major peaks of cysteine desulfurase activity (Fig. 8*A*). Fractions corresponding to the last and largest cysteine desulfurase peak (fractions 20–27) contained the protein that reacted well with the anti-EhNifS and anti-CS antibodies (Fig. 8*B*). In contrast, fractions corresponding to the first and second cysteine desulfurase peaks did not react with anti-EhNifS antibody but reacted with anti-MGL and anti-CS antibodies, respectively. rEhNifS was fractionated under the same conditions and showed a single peak eluted at a slightly lower ionic strength (0.5 ml earlier elution volume) than the native EhNifS (Fig. 8*C*), which is consistent with the fact that recombinant histidine-tagged EhNifS has a slightly higher pI (6.15) than the native protein (5.9). These results suggest that the third dominant cysteine desulfurase peak of the parasite lysate represents activity mainly attributable to native EhNifS.

Heterologous Expression of the Amebic NifS and NifU in the isc/suf-Mutant E. coli Strain—To assess the *in vivo* role of EhNifS and EhNifU, we attempted heterologous complementation of an *E. coli* mutant UT109 in which the chromosomal *isc* and *suf* operons were deleted. This strain was lethal unless we provided the *suf* or *isc* operon in a complementing plasmid carrying a temperature-sensitive replicative origin.[7] At the restrictive temperature, introduction of the *E. coli isc* or *suf* operon in a complementing plasmid carrying a temperature-insensitive replicative origin complemented the growth defects of the UT109 strain under both the aerobic and anaerobic conditions (Fig. 9). In contrast, coexpression of EhNifS and EhNifU rescued the growth of UT109 only under the anaerobic, not aerobic, conditions at the restrictive temperature. Thus, the amebic NifS and NifU are apparently necessary and sufficient for the Fe-S cluster formation under anaerobic conditions in this heterologous system. Although CS and MGL showed cysteine desulfurase activity *in vitro*, coexpression of CS1 or MGL2, together with EhNifU, did not complement the growth defects of UT109 under either aerobic or anaerobic conditions (data not shown).

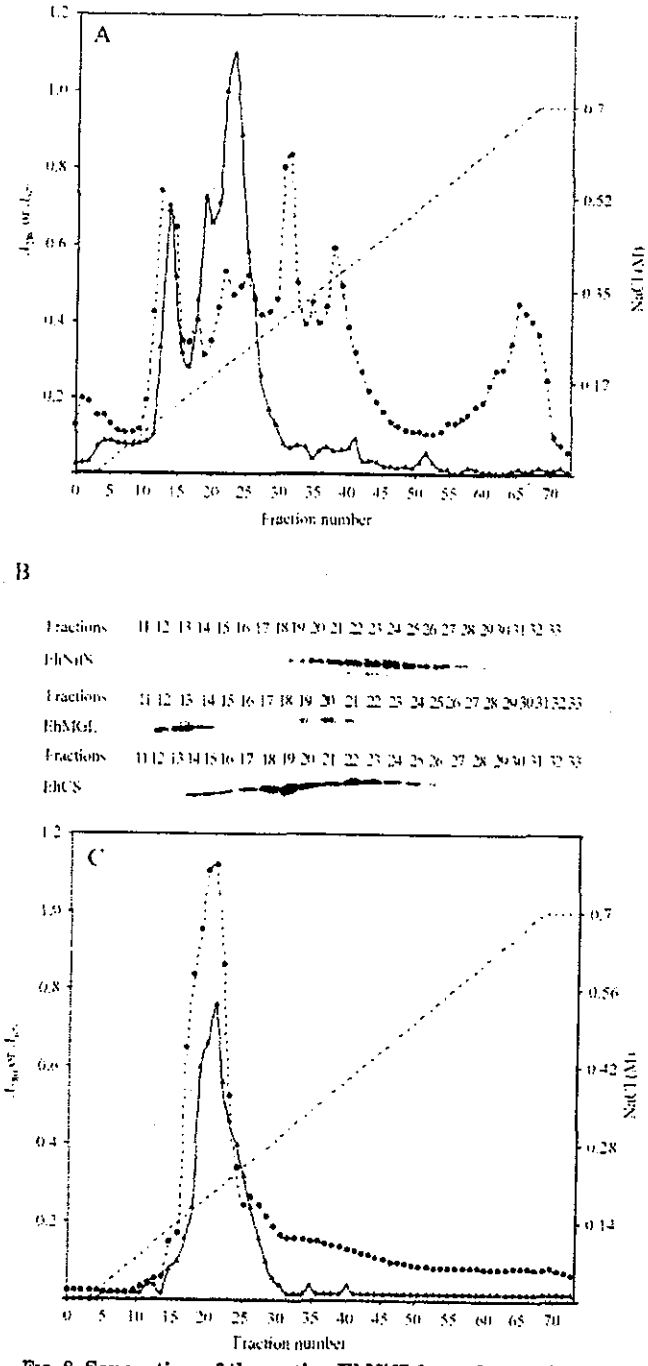

FIG. 8. **Separation of the native EhNifS from the *E. histolytica* trophozoites and rEhNifS with Mono Q anion exchange chromatography.** *A*, elution profile of the native EhNifS. The total lysate of *E. histolytica* trophozoites was separated on the anion exchange column at pH 8.0 with a linear gradient of NaCl (*dashed line*) (0–0.7 M). *Triangles* and an *unbroken line* depict cysteine desulfurase activity, shown as A_{670}, *Circles* and a *broken* line show A_{280}. *B*, immunoblots of each fraction with anti-EhNifS, MGL, and CS antibodies. *C*, elution profile of the recombinant EhNifS. The rEhNifS protein was fractionated under the same conditions as in *A*. *Triangles* and an *unbroken line* show cysteine desulfurase activity. *Circles* and a *broken line* represent A_{280}. A *dashed line* represents NaCl concentrations of a linear gradient.

DISCUSSION

We have identified and characterized two necessary and sufficient components, NifS and NifU, of the NIF-like system for the assembly of Fe-S clusters in a human intestinal protozoan anaerobe. As far as we are aware, this is the first demonstration of the NIF-like system in eukaryotes. Despite a thorough search of the *E. histolytica* genome database, no other proteins that were shown to be involved in ISC/SUF systems of other organisms were found, suggesting that this parasite possesses the NIF-like system as a sole and non-redundant system for the biosynthesis of all Fe-S proteins. Because *E. histolytica*

[6] V. Ali and T. Nozaki, unpublished data.
[7] U. Tokumoto and Y. Takahashi, manuscript in preparation.

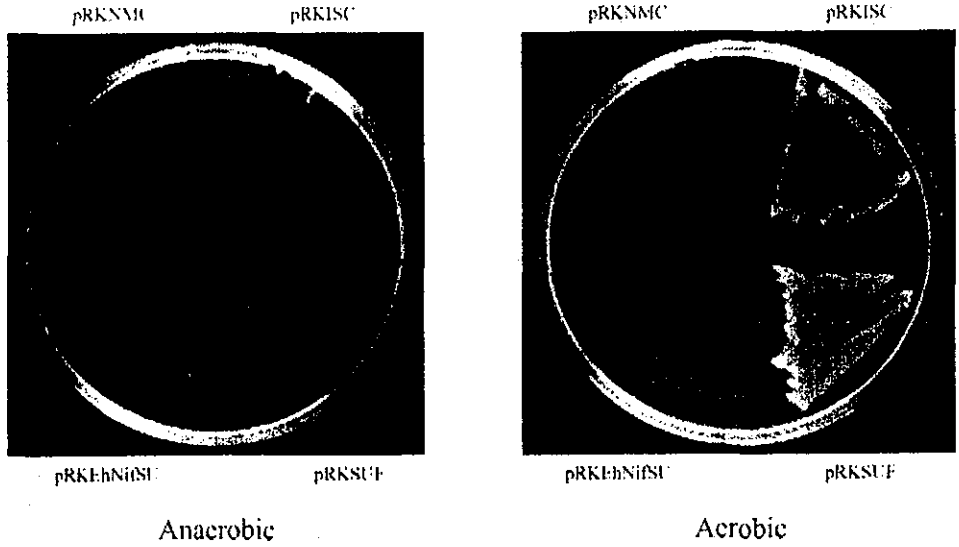

FIG. 9. **Functional complementation of the *isc/suf*-mutant *E. coli* strain by coexpression of EhNifS and EhNifU under anaerobic conditions.** pRKEhNifSU, pRKISC, or pRKSUF, which contains *E. histolytica* EhNifS and EhNifU, *E. coli iscSUA-hscBA-fdx*, or *E. coli sufABCDSE* operon, respectively, in pRKNMC, or pRKNMC alone was introduced into *E. coli* strain UT109 [Δ(*iscSUA-hscBA*)::Km^r, Δ(*sufABCDSEU*)::Gm^r] as described in "Experimental Procedures." The transformants were cultivated at the restrictive temperature under either aerobic or anaerobic conditions.

does not possess nitrogenase and is incapable of nitrogen fixation, the presence of the *NIF-like system* and the lack of other systems in this organism reinforce the premise that the NIF system is not specific for the Fe-S cluster formation of nitrogenase but is involved in the Fe-S cluster assembly for nitrogenase and non-nitrogenase proteins, as proposed for the NIF-like system in *H. pylori* (13). Our *in vivo* complementation of a temperature-dependent growth defect of the *E. coli isc/suf* mutant strain by expression of a heterologous NIF-like system indicates that the NIF-like system plays an interchangeable role in the Fe-S cluster assembly of non-nitrogenase proteins with the ISC or SUF system under anaerobic conditions. Despite common catalytic and scaffold mechanisms shared by the NIF, ISC, and SUF systems, there are a number of differences among these systems (10); the ISC and SUF systems appear to be considerably more complex than the NIF system. For example, heat-shock-cognate (Hsc) proteins have been suggested to have chaperone-like functions in the ISC system for the formation of transient Fe-S clusters or insertion into various target proteins in bacteria and yeast (7, 26, 30, 50, 51). Our *in vivo* complementation study revealed that the NIF-like system does not require any additional component other than NifS and NifU for Fe-S cluster assembly under anaerobic conditions. However, it is also possible that as yet unidentified proteins that remain in the *isc/suf*-mutant strain of *E. coli* function together with the exogenous NifS and NifU. It is also conceivable that the NIF-like system is shared by other anaerobic parasitic organisms. However, two other well-characterized anaerobic protozoan parasites *G. lamblia* and *T. vaginalis* appear to possess the ISC and lack the NIF system (32, 34). Thus, the presence of the NIF-like system is likely unique to *E. histolytica*, which might be attributable to a rare horizontal gene transfer from a NIF-like-containing prokaryotic organism (see below).

Several lines of evidence support close kinship between the amebic NifS and NifU and their homologs from ϵ-proteobacteria. First, phylogenetic analyses indicate that *E. histolytica* and ϵ-proteobacteria represent an independent clade well separated from other NifS and NifU homologs. Second, this close phylogenetic association is also supported by the common insertions and deletions of amino acids shared by NifS and NifU from these organisms. Third, the multimeric structure of the amebic and *H. pylori* NifU is identical (*i.e.* tetramer), whereas NifU from *A. vinelandii* and IscU from *E. coli* and yeast form a dimer. Fourth, UV/visible absorption spectra and specific activity of EhNifS were comparable to the *H. pylori* NifS but notably different from *A. vinelandii*. These data suggest that amebic *nif*-like genes were likely obtained from an ancestral organism currently represented by ϵ-proteobacteria by lateral gene transfer, as suggested for other metabolic enzymes that are proposed to have been transferred from Archaea and/or bacteria by a similar mechanism (52–54).

Fractionation of the crude extract of *E. histolytica* by anion-exchange chromatography revealed that at least three groups of enzymes, CS, MGL, and NifS, contributed to cysteine desulfurase activity, *i.e.* activity to mobilize the sulfur or sulfide from L-cysteine, and thus possibly provide sulfur for Fe-S cluster synthesis. Although both CS and MGL showed cysteine desulfurase activity[6] (see also "Results" and Ref. 16 for *E. coli* CS) and also *in vitro* activity to convert an apo form of recombinant amebic $[4Fe\text{-}4S]^{2+}$ ferredoxin (53, 55) into a holo form,[6] we argue that EhNifS is the sole protein that functions in Fe-S cluster biosynthesis *in vivo*. Expression of CS or MGL (*i.e.* EhCS1 or EhMGL2), when coexpressed with EhNifU, did not complement the Fe-S cluster formation of the *isc/suf*-mutant strain of *E. coli* (data not shown). This reinforces the previous observation on *E. coli* cysteine synthase A, B, and γ-cystathionase (16) and indicates that the *in vitro* conversion assay of apo Fe-S protein does not reflect *in vivo* function.

We did not demonstrate in the present study the species of the temporal Fe-S cluster (*i.e.* $[2Fe\text{-}2S]^{2+}$ or $[4Fe\text{-}4S]^{2+}$) that formed on EhNifU in addition to the stable $[2Fe\text{-}2S]^{2+}$ cluster shown in Fig. 6. However, it is conceivable, by analogy to NifU from *A. vinelandii* involved in the Fe-S cluster formation of nitrogenase, that amebic NifU functions as an intermediate site for the transient $[2Fe\text{-}2S]^{2+}$ cluster assembly (12). The putative labile $[2Fe\text{-}2S]^{2+}$, if present, was likely lost during purification under aerobic conditions. We also speculate that the transition of Fe-S clusters on EhNifU may occur under anaerobic conditions; one $[4Fe\text{-}4S]^{2+}$ cluster may be formed from two $[2Fe\text{-}2S]^{+2}$ clusters, as shown for *Azotobacter* IscU (5). Because the amebic NifU forms a tetramer, the mechanism of the $[4Fe\text{-}4S]^{2+}$ cluster formation from $[2Fe\text{-}2S]^{2+}$ on NifU may differ from *Azotobacter* NifU, which exists as a dimer. Because